New insights into lake responses to rapid climate change: the Younger Dryas in Lake Gościąż, central Poland

DANIELA MÜLLER (iD), RIK TJALLINGII, MATEUSZ PŁÓCIENNIK (iD), TOMI P. LUOTO, BARTOSZ KOTRYS, BIRGIT PLESSEN, ARNE RAMISCH, MARKUS J. SCHWAB, MIROSŁAW BŁASZKIEWICZ, MICHAŁ SŁOWIŃSKI AND ACHIM BRAUER

The sediment profile from Lake Gościąż in central Poland comprises a continuous, seasonally resolved and exceptionally well-preserved archive of the Younger Dryas (YD) climate variation. This provides a unique opportunity for detailed investigation of lake system responses during periods of rapid climate cooling (YD onset) and warming (YD termination). The new varve record of Lake Gościąż presented here spans 1662 years from the late Allerød (AL) to the early Preboreal (PB). Microscopic varve counting provides an independent chronology with a YD duration of 1149+14/–22 years, which confirms previous results of 1140±40 years. We link stable oxygen isotopes and chironomid-based air temperature reconstructions with the response of various geochemical and varve microfacies proxies especially focusing on the onset and termination of the YD. Cooling at the YD onset lasted ~180 years, which is about a century longer than the terminal warming that was completed in ~70 years. During the AL/YD transition, environmental proxy data lagged the onset of cooling by ~90 years and revealed an increase of lake productivity and internal lake re-suspension as well as slightly higher detrital sediment input. In contrast, rapid warming and environmental changes during the YD/PB transition occurred simultaneously. However, initial changes such as declining diatom deposition and detrital input occurred already a few centuries before the rapid warming at the YD/PB transition. These environmental changes likely reflect a gradual increase in summer air temperatures already during the YD. Our data indicate complex and differing environmental responses to the major climate changes related to the YD, which involve different proxy sensitivities and threshold processes.

Daniela Müller (daniela.mueller@gfz-potsdam.de) and Achim Brauer, Section Climate Dynamics and Landscape Evolution, GFZ German Research Centre for Geosciences, Telegrafenberg, Potsdam 14473, Germany and Institute of Geosciences, University of Potsdam, Karl-Liebknecht-Str. 24–25, Potsdam 14476, Germany; Rik Tjallingii, Birgit Plessen, Arne Ramisch and Markus J. Schwab, Section Climate Dynamics and Landscape Evolution, GFZ German Research Centre for Geosciences, Telegrafenberg, Potsdam 14473, Germany; Mateusz Płóciennik, Department of Invertebrate Zoology and Hydrobiology, University of Łódź, Banacha st. 12/16, Łódź 90-237, Poland; Tomi P. Luoto, Faculty of Biological and Environmental Sciences, Ecosystems and Environment Research Programme, University of Helsinki, Niemenkatu 73, Lahti 15140, Finland; Bartosz Kotrys, Polish Geological Institute - National Research Institute, Pomeranian Branch in Szczecin, Wieniawskiego 20, Szczecin 71-130, Poland; Mirosław Błaszkiewicz and Michał Słowiński, Department of Environmental Resources and Geohazards, Institute of Geography and Spatial Organization, Polish Academy of Sciences, Kopernika 19, Toruń 87-100, Poland; received 30th June 2020, accepted 6th November 2020.

Lakes are considered as sentinels of climate change since they respond immediately, but also incorporate effects of climate change within the catchment (Adrian *et al.* 2009, 2016). However, lake responses to climate change are complex, due to the involvement of tightly coupled physical, chemical and biological processes that operate on a wide range of time scales from days to millennia (Ramisch *et al.* 2018). Numerous studies based on modern observations address how different compartments of lake systems respond to climate change (e.g. Adrian *et al.* 2016). However, there are still synergistic and complex lake response mechanisms that are not fully understood (Havens & Jeppesen 2018). In particular, ecosystem changes to abrupt climate change yet remain elusive (Botta *et al.* 2019).

Since major hemispheric climatic shifts did not occur during historical times, we need to apply a forensic approach and investigate these climatic changes in lake sediments in the geological past. An ideal time interval for such investigations is the Younger Dryas (YD) cold period at the end of the Last Glaciation, which marks the last major climate fluctuation in the Northern Hemisphere (e.g. Brauer *et al.* 2008; Denton *et al.* 2010; Clark *et al.* 2012; Rach *et al.* 2014). The YD is characterized by pronounced seasonality with strong winter cooling (Isarin *et al.* 1998; Denton *et al.* 2005) and relatively mild but short summers (Schenk *et al.* 2018). Changes in seasonality are considered crucial for lake system response, because spring and early summer is a critical time window for the timing and rates of overturn and related biological effects (Peeters *et al.* 2007; Adrian *et al.* 2016). Therefore, varved lake sediment records with seasonal time resolution are most suitable recorders of seasonal effects. However, there are only a few lake records reported that are completely varved throughout the YD and document the rapid climatic and environmental changes at the YD transitions with seasonal resolution. In Europe, these lakes include Lake Gościąż (Ralska-Jasiewiczowa *et al.*

1987, 1998b; Goslar *et al.* 1989), Meerfelder Maar (Brauer *et al.* 1999) and palaeolake Rehwiese (Neugebauer *et al.* 2012). Pioneer studies were carried out on the Lake Gościąż varves starting in the late 1980s (Ralska-Jasiewiczowa *et al.* 1987; Goslar *et al.* 1989) that revealed fundamental results on YD varve dating, radiocarbon calibration and vegetation change (Goslar *et al.* 1989; Ralska-Jasiewiczowa *et al.* 1998b). Based on varve counting of Lake Gościąż sediments even changes in atmospheric radiocarbon concentrations during the YD were determined (Goslar *et al.* 1995, 1999). In addition, regional vegetation changes related to the YD were reconstructed in great detail (Goslar *et al.* 1992; Ralska-Jasiewiczowa *et al.* 1992, 1998b, 2003). A truly seminal study was the reconstruction of environmental changes at 1–4 year resolution during the transition to the Holocene (Ralska-Jasiewiczowa *et al.* 2003) based on pollen and geochemical data. We adopt the principal approach of this study, but include novel analytical methods including continuous X-ray fluorescence (XRF) core scanning and μ-XRF mapping, continuous microfacies analyses and chironomid-based temperature reconstructions. We further extend the time interval to the entire YD, including the transition from the Allerød (AL) into the YD. This study is part of a larger project re-visiting the entire Holocene and Lateglacial sediment record from Lake Gościąż (Bonk *et al.* 2021). The main goal of this study is to compare the mechanisms and dynamics of lake system responses to major cooling and warming events. We distinguish between temperature and environmental proxies to decipher in detail the succession of lake-internal and catchment responses to large-scale temperature changes.

Study area

Lake Gościąż (GOS) is located about 80 km WNW of Warsaw in central Poland (latitude 52°35'N, longitude 19°21'E; Fig. 1). It is situated at 64.3 m a.s.l. and has a surface area of 41.7 ha, a maximum water depth of 22 m and a catchment area of 588 ha. GOS is the largest lake of the Na Jazach four lake system, which is today connected by the Ruda stream, draining into the Vistula River (since 1970 to the Włocławek Reservoir). The lake is predominantly groundwater fed with 80–90% of present day inflow from groundwater (Gierszewski 1993; Giziński *et al.* 1998; Rozanski *et al.* 2010). GOS is a kettlehole lake within a subglacial channel that formed during the Last Glaciation. The last ice-sheet advance of the Scandinavian Ice Sheet (Late Weichselian ice sheet) in this area occurred during the Poznań phase (20–19 cal. ka BP; Marks *et al.* 2016), leading to the formation of subglacial channels and burial of dead ice during the final stage of ice-sheet advance and later recession (Błaszkiewicz *et al.* 2015). Melting of buried dead ice blocks resulted in formation of kettlehole lakes like Lake Gościąż. Finely laminated lacustrine sediments in this lake are preserved

since the late Allerød (Ralska-Jasiewiczowa *et al.* 1987, 1998b; Goslar *et al.* 1989).

The lake catchment consists primarily of glacifluvial sediments and features also aeolian forms (e.g. dunes; Rychel *et al.* 2018; Kruczkowska *et al.* 2020). Present day vegetation predominantly is composed of pine forests and subordinated also by aquatic, reed swamp, mire, meadow, grassland, scrub, ruderal and segetal communities (Kępczyński & Noryśkiewicz 1998). The monthly mean surface air temperature ranges from −2.8 °C in January to +18 °C in July (Wójcik & Przybylak 1998; Rozanski *et al.* 2010), while the annual mean surface air temperature is 8.2 °C (Rozanski *et al.* 2010). The monthly mean precipitation ranges from 25.6 mm (February) to 82.5 mm (July) with an annual mean of 540 mm (Wójcik & Przybylak 1998). Westerly winds prevail in the area of the lake (Wójcik & Przybylak 1998).

Material and methods

Coring

Coring was conducted with an UWITEC Piston Corer during two coring campaigns in 2015 (GOS15) and 2018 (GOS18) (Fig. 1). In 2015, three parallel sediment cores (A, B and C) were obtained from the southern section of the deepest part of the lake basin at 21.3–21.5 m water depth. Since the sediments were disturbed by a ~2-m-thick mass movement deposit in the lowermost part of the cores (Fig. S1), five new parallel sediment cores (D, E, G, H, I) were obtained in 2018 from the northwestern part of the deep basin at 19.5–21.6 m water depth, because this location is more distal with respect to the mass-wasting event that caused the major mass movement deposit. A composite profile with a total length of 1897 cm was established for the finely laminated lacustrine sediments using cores GOS15-A, -B, -C and GOS18-H (Bonk *et al.* 2021). This study focuses on the lowermost laminated sediments between 1717.8 and 1897 cm depth covering the beginning of limnic sedimentation from the late Allerød (AL) to the early Preboreal (PB) (see Table S1 and Fig. S1).

Microfacies analyses

Microfacies analyses were performed on 26 overlapping large-scale thin sections prepared from 10-cm-long freeze-dried and resin impregnated sediment slices (Brauer & Casanova 2001). The analyses included varve counting and measurements of varve and sublayer thickness based on determination of varve composition, structure and boundaries. We defined a varve quality index (VQI) from VQI 0 (no varve preservation) to VQI 3 (perfect varve preservation with sharp boundaries) that was allocated to each varve. Microscope analysis was conducted with an Axioplan 2 and Axiolab pol imaging microscope with parallel and polarized light using
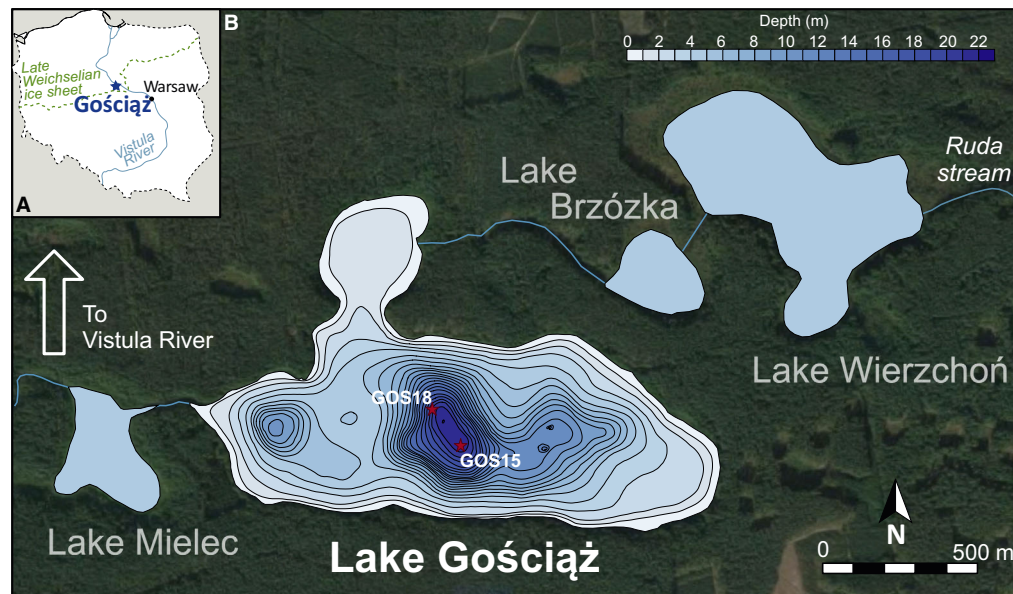
Fig. 1. A. Overview map of Poland including location of Lake Gościąż, Warsaw, the Vistula River and the maximum extent of the Late Weichselian ice sheet according to Ralska-Jasiewiczowa *et al.* (1998c). B. Aerial photograph of the study site, location of Lake Gościąż as part of the Na Jazach four lake system and lake bathymetry. Coring sites in 2015 (GOS15) and 2018 (GOS18) are marked with red stars.

magnifications between 50 and 400×. Thin section photographs were taken with an Olympus BX53F microscope, connected to an Olympus DP72 camera.

Chronology

A floating varve chronology was established by microscopic layer counting on large-scale thin sections. Counting uncertainties are calculated from comparing three independent counts. The count C2 is considered as most accurate, because layer thickness was precisely measured (Martin-Puertas *et al.* 2014) and was thus used as a reference. The counting difference from the other two counts (C1, C3) was calculated for each thin section and summed up. It was distinguished between negative differences (fewer counted varves; under-counting) and positive differences (more counted varves; over-counting). Maximum over- and undercounts are given as counting uncertainty. The varve chronology presented in this study is an integrated part of a long Holocene floating chronology including more than 10 000 varves that has been anchored to the absolute time scale through radiocarbon dating and age modelling with Bacon (Bonk *et al.* 2021).

XRF element scanning

Non-destructive XRF core scanning was performed on smoothed surfaces of fresh sediment cores using an ITRAX XRF Core Scanner (Croudace *et al.* 2006) at GFZ Potsdam. Measurements were obtained every 200 µm using a Cr-X-ray source (30 kV, 30 mA) and 10-s measurement time. Element intensities are acquired in counts per second (cps) and displayed as log-ratios that resemble variations of geochemical composition (Tjallingii *et al.* 2007; Weltje & Tjallingii 2008; Weltje *et al.* 2015).

For direct comparison of the sediment composition with microfacies analyses, µ-XRF element mapping was performed on two impregnated sediment blocks that were also used for thin section preparation. The two selected samples cover the onset and termination of the YD. Element mapping was conducted with a Bruker M4 Tornado µ-XRF scanner that is equipped with a Rh X-ray source (50 kV, 600 µA) and poly-capillary X-ray optics generating a spot size of approximately 20 µm. Measurements were obtained every 50 µm using a 30-ms measurement time. Normalized element intensities are used to visualize relative element abundances as 2D maps. Both XRF analyses are of sub-annual resolution.

Chironomid analysis and air temperature reconstruction

Chironomidae subfossils were collected from a total of 233 samples from the composite profile. Samples that contained fewer than 50 head capsules (hc) as required for robust reconstruction (Quinlan & Smol 2001) were merged and also labelled as 'samples'. For this reason, the sample resolution of our temperature reconstruction ranges from 0.5 to 6 cm and the temporal resolution between 3 and 68 varves per sample. For a total of 31 samples the required number of 50 hc was not obtained even after sample merging (Table S2). Nevertheless, these samples were still included in the reconstruction because either the hc number was very close to 50 and/ or the results of temperature reconstruction were consistent with the results based on adjacent samples

in which the number of hc reached at least 50. The lowest hc number used for temperature reconstruction is 30 and the highest is 170 with a mean of 61 hc per sample. Two different training sets were used for mean July air temperature (MJAT) reconstructions – the Swiss-Norwegian-Polish Training Set (SNP TS) (Kotrys *et al.* 2020) and the East European TS (EE TS) (Luoto *et al.* 2019). The SNP TS includes 357 lakes, 134 taxa and covers the 3.5–20.1 °C temperature range. The EE TS includes 212 lakes, 142 taxa and covers the 11.3–20.1 °C temperature range. Both TS use the weighted averaging-partial least squares transfer function (WA-PLS). The SNP TS root mean squared error of prediction (RMSEP) and R^2_{jack} for the WA-PLS component 3 are 1.39 °C and 0.91, respectively, and the EE TS RMSEP and R^2_{jack} for the WA-PLS component 2 equals 0.88 °C and 0.88, respectively (Luoto *et al.* 2019; Kotrys *et al.* 2020). The temperature reconstructions were carried out with C2 software (Juggins 2007).

Stable isotopes

Stable isotopes of oxygen in carbonates ($\delta^{18}O_{carb}$) and of carbon in bulk organic matter ($\delta^{13}C_{org}$) were determined on bulk sediment samples contiguously taken at 1-cm resolution, except for the sections 1737.4–1757.4 and 1880.2–1891.7 cm depth, which were sampled at 0.5-cm resolution. The temporal resolution of the samples varies between ~4–14 varves cm^{-1} in the intervals from 1717.4–1737.4 and 1757.4–1872.3 cm, ~18–23 varves cm^{-1} from 1891.7 to 1897 cm and ~8–24 varves cm^{-1} in the intervals from 1737.4–1757.4 and 1880.2–1891.7 cm. All samples were freeze-dried, manually ground and homogenized. Measurement of $\delta^{18}O_{carb}$ was performed by an automated carbonate device (KIEL IV) connected to a MAT253 Isotope Ratio Mass Spectrometer (IRMS, Thermo Fisher Scientific). $\delta^{13}C_{org}$ was determined after *in situ* de-carbonization in Ag-capsules first with 3% and second with 20% HCl using an automatic elemental analyser (NC2500 Carlo Erba) coupled with a ConFlow III interface on a DELTAplusXL IRMS. Both isotope compositions are given relative to the Vienna PeeDee Belemnite (VPDB) standard. $\delta^{18}O_{carb}$ was calibrated against NBS-19 and an internal reference sample (C1), while $\delta^{13}C_{org}$ was calibrated against IAEA-CH7 and an elemental isotope standard (Urea) and was proved with an internal soil reference sample (Boden3) and Pepton (PEP). Standard errors are 0.06‰ for $\delta^{18}O_{carb}$ and 0.2‰ for $\delta^{13}C_{org}$.

Results

Lithology

A detailed lithological description of the entire new composite profile is given by Bonk *et al.* (2021). This study focuses on the interval between 1717.8 and 1897 cm (Fig. 2), which comprises lithozones 5a and 5b (1749–1897 cm) and the lower 31.2 cm of lithozone 4 (1717.8–1749 cm) (Fig. S1). Briefly summarized, a sharp boundary marks the transition between the basal glacial sands of lithozone 6 and the finely laminated lacustrine sediments of lithozone 5. The transition between lithozones 5b and 5a at ~1885 cm is marked by a colour change of the couplets from light brown and beige to brown and beige. A ~7-cm-thick grey-brown graded layer occurs at 1879.6 cm, which is covered by a discrete grey silt-clay layer of ~2 mm thickness. This discrete layer is similar to the layer covering the thick slump deposits observed in cores located closer to the southern shore. Therefore, we interpret the graded layer as distal deposit of a large mass-wasting event. The transition from lithozone 5 to lithozone 4 at 1748.6 cm depth is characterized by a sharp and distinct colour change due to the sudden appearance of dark sublayers. The upper boundary of our study interval was defined at a succession of two varves with thick calcite sublayers that form a discrete marker horizon.

Chronology and Younger Dryas definition

The varve chronology of our study interval is the lowest part of a new floating varve chronology for Lake Gościąż that reaches from the Lateglacial to the Late Holocene and has been anchored to the absolute time scale by age modelling and radiocarbon dating (Bonk *et al.* 2021). The chronology of our study interval includes the lowest 1662+14/–22 varves of this overall chronology and comprises the period from the onset of lacustrine sedimentation at 12 834+134/–235 to 11 173+123/–204 cal. a BP (Fig. 2A). The uncertainty for the absolute ages is due to radiocarbon age modelling of a non-varved interval between ~1000 and 2600 cal. a BP (Bonk *et al.* 2021). In comparison, internal varve counting uncertainty in the study interval is very low due to the mostly excellent varve preservation (mean VQI of 2.6).

In the previous study of Lake Gościąż, the YD boundaries have been defined in the centre of the major shifts in $\delta^{18}O$ of bulk carbonate, nearly coinciding with vegetation changes (Ralska-Jasiewiczowa *et al.* 1992). We adopt this YD definition, since our record exactly reproduces the published $\delta^{18}O_{carb}$ YD signal (Kuc *et al.* 1998) allowing precise correlation of the YD boundaries (Fig. 2B). According to this definition the YD is dated at 12 620+133/–231 to 11 470+126/–206 cal. a BP in our age model. The late Allerød encompasses 215 varves (1886.4–1897 cm), the YD 1149 varves (1748.5–1886.4 cm) and the early Preboreal 298 varves (1717.8–1748.5 cm).

Microfacies analyses

The highest VQI is obtained for the PB (2.8) and mostly during the early YD a few intervals with lower VQI are found (Fig. 4).
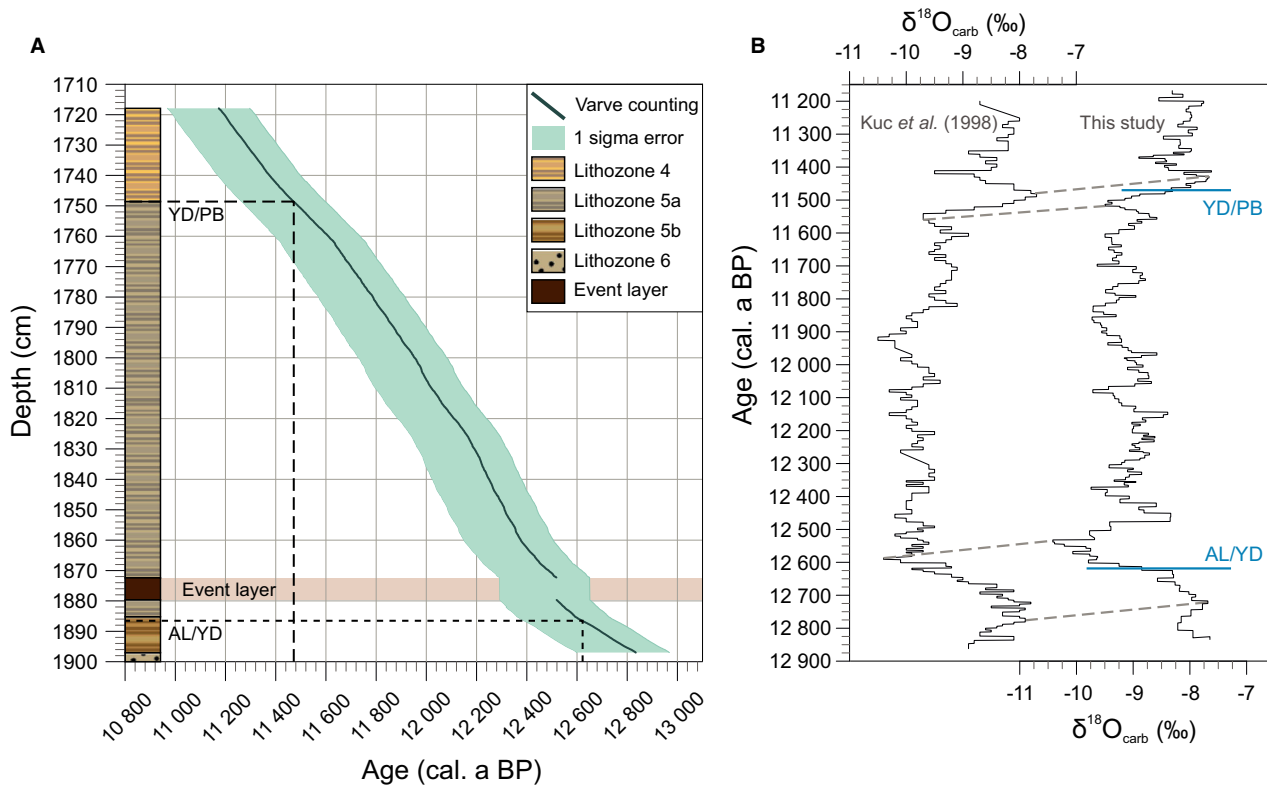
Fig. 2. A. Floating varve chronology for our study interval. Absolute ages are derived from age modelling and radiocarbon dating (Bonk *et al.* 2021), causing the largest portion of age uncertainties. The varve counting uncertainty is lower (+14/–22) and not possible to show in this figure. Lithological profile on the left. YD/PB = Younger Dryas/Preboreal; AL/YD = Allerød/Younger Dryas. B. Correlation of stable oxygen isotope data from Lake Gościąż with independent chronologies: previous study (Kuc *et al.* 1998) on the left and this study on the right. Dashed grey lines mark the correlation of both curves. Positions of the YD boundaries as defined in our study are marked with blue lines.

Varve types. – The studied sediment section consists primarily of autochthonous material and two calcite varve microfacies types are distinguished: calcite-organic varves (type I) and diatom-calcite varves (type II) (Fig. 3). Calcite-organic varves appear slightly different in the lower and upper parts of the study interval. Thus, two subtypes (Ia and Ib) are differentiated.

Varve type I: calcite-organic varves. – The calcite-organic microfacies (subtype Ia) occurs between 1885.4–1897 cm (12 597–12 834 cal. a BP; Fig. 3) in 239 varves and comprises up to three sublayers. The sedimentation cycle starts with a sublayer of white idiomorphic calcite grains of 10–20 μm in size, which rarely includes a few scattered quartz grains. The following sublayer consists of fine-grained (2–5 μm) brown-yellowish and rounded grains resembling Mn-Fe-carbonates and rarely includes pyrite framboids. This sublayer only occurs in 58 varves primarily in the lower part of this interval. The sedimentation cycle terminates with an amorphous organic matter sublayer, which includes scattered brown-yellowish carbonate grains that form the sublayer below.

The calcite-organic microfacies (subtype Ib) appears in 295 varves from 1748.6 cm until the top of the study

interval (11 472–11 173 cal. a BP; Fig. 3). Similar to subtype Ia, the ideal sedimentation cycle encompasses three sublayers including (i) an idiomorphic calcite sublayer at the base followed by (ii) an amorphous organic matter sublayer, and (iii) a sublayer of brown-yellowish rounded carbonate, which however, appears only in 122 varves of this facies type. The main difference to subtype Ia is that (i) the idiomorphic calcite crystals in the basal sublayer are generally finer grained (2–10 μm), (ii) the amorphous organic matter sublayer frequently includes also scattered calcite and vivianite grains, and (iii) the brown-yellowish carbonate sublayer is generally thinner and appears after the amorphous organic matter sublayer.

Varve type II: diatom-calcite varves. – The diatom-calcite microfacies is developed in 1128 varves between 1748.6–1885.4 cm (11 473–12 596 cal. a BP; Fig. 3) and has a complex and variable structure with up to six sublayers (SL1 to SL6) as described in stratigraphical order from the base to the top in the following:

1 Rounded brown-yellowish carbonate with grain sizes <3 μm that resemble Mn-Fe-carbonates.
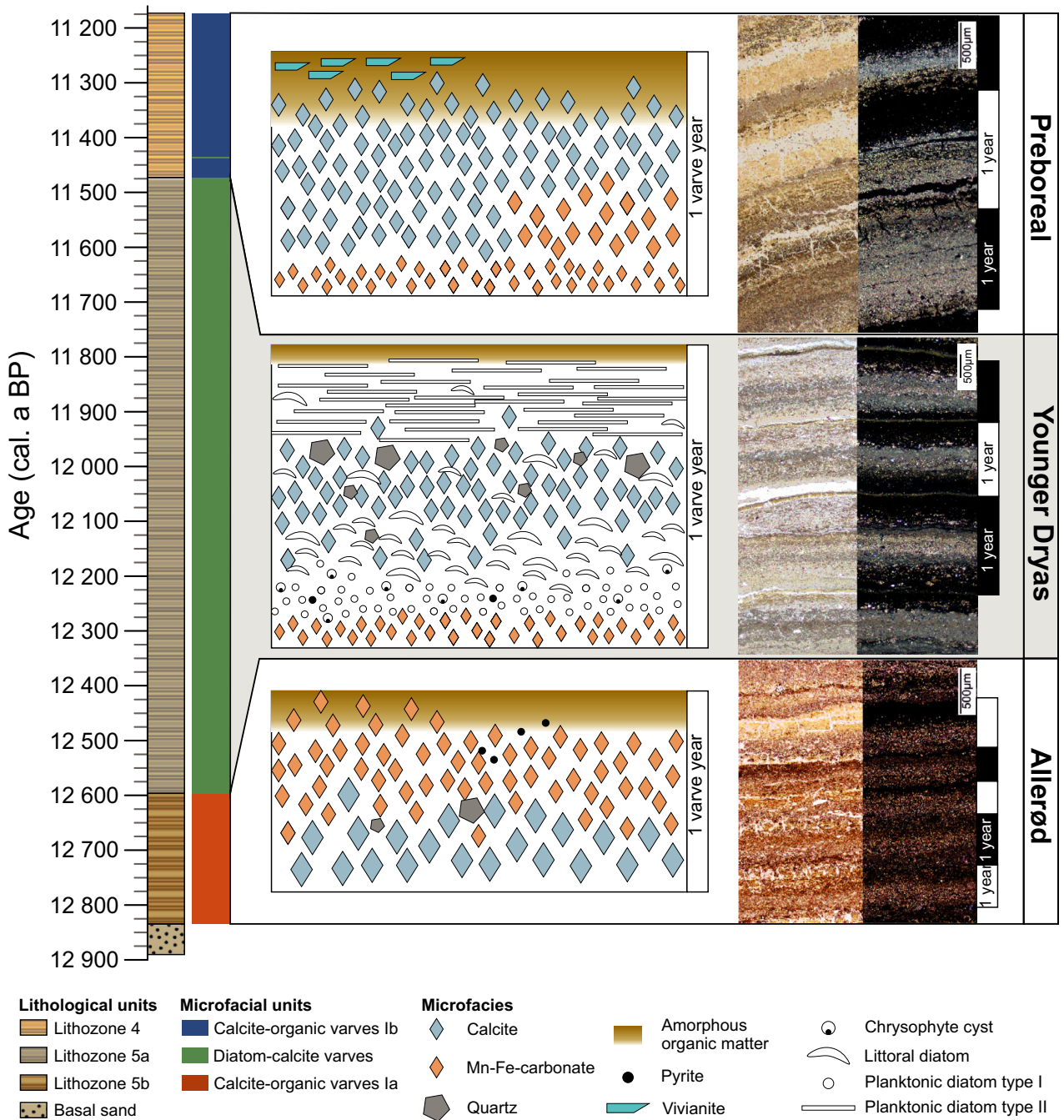
Fig. 3. Left: lithology and varve type distribution over the profile. Centre: microfacies models of calcite-organic varves within the Allerød (subtype Ia) and the Preboreal (subtype Ib), as well as diatom-calcite varves (Younger Dryas). Right: thin section pictures of the different microfacies types (left: non-polarized light, right: polarized light).

2 Planktonic diatoms and a few chrysophyte cysts, interspersed with littoral diatoms and rare pyrite framboids.

3 Primarily diatoms with some patches of white-yellowish idiomorphic calcite. The diatom assemblage consists either of littoral diatoms, planktonic diatoms or a mixture of both. Rare chrysophyte cysts and silt-sized quartz grains occur.

4 Primarily patches of white-yellowish idiomorphic calcite and sub-ordinated littoral diatoms and a few scattered silt-sized quartz grains. In 62 varves a discrete sublayer of detrital quartz of 0.09–0.64 mm thickness (mean 0.3 mm) develops on top of SL4 (Fig. 4).

5 Predominantly planktonic diatoms and rarely littoral diatoms. In some varves a few patches of amorphous

organic matter and white-yellowish idiomorphic calcite occur.

6 Amorphous organic matter with a few brown-yellowish rounded Mn-Fe-carbonate grains included in some varves.

The frequency of discrete quartz-rich sublayers in SL4 varies within the record (Fig. 4). Between 1885.4–1862.4 cm (12 595–12 400 cal. a BP) and 1834.8–1777.5 cm (12 220–11 765 cal. a BP) they occur every 20 to 25 years, while between 1862.4 and 1834.8 cm (12 400–12 220 cal. a BP) these sublayers appear more frequently and occur about every 6 years.

Varve thickness. – In addition to total varve thickness, we also measured individual sublayer thicknesses for all varves (Figs 4, S2). Only calcite and amorphous organic sublayers occur in all varve types, while diatom sublayers are present only in varve type II. We further calculated the coefficient of variation for the AL, YD and PB as an indication of interannual variability (Fig. 5).

Calcite-organic varves (subtype Ia) deposited during the late Allerød have a mean varve thickness of 0.49 mm, which is the lowest of the study interval. A low coefficient of variation (28.3%) indicates low interannual variability of varve thickness (Fig. 5).

The mean varve thickness of 1.14 mm for diatom-calcite varves formed during the YD is more than doubled compared to the AL. The main reason for the varve thickness increase is the presence of diatom sublayers of up to 3 mm thickness (Fig. 4). A slight increase in the re-suspended calcite sublayer further contributes to increased thickness of YD varves. A more detailed view reveals that the period of thickest varves (mean thickness of 1.32 mm) is confined to ~12 375 to 11 635 cal. a BP, mainly because of the frequent occurrence of thick diatom sublayers between ~12 380 and 11 935 cal. a BP. A pronounced decrease in diatom sublayers occurs around 11 700 cal. a BP. In the early phase of the YD, varve thickness shows an increasing trend with occasional occurrence of thicker varves (mean thickness of 0.82 mm), whereas in the last phase of the YD the mean varve thickness of 0.83 mm is similar, but varves thicker than ~1.5 mm do not occur anymore. In general, the interannual variability of varve thickness is distinctly enlarged during the YD as shown by the coefficient of variation of 49.4% (Fig. 5).

Mean varve thickness of calcite-organic varves (subtype Ib) formed during the PB is 1.03 mm, which is only slightly lower than the YD mean and even higher than in the late YD (~11 635–11 470 cal. a BP). The reason for the increase of PB varve thickness at the YD/PB transition is the deposition of thick amorphous organic sublayers (Fig. 4). The interannual variability of varve thickness (coefficient of variation 29.9%) is similar to the AL and distinctly different from the YD (Fig. 5).

XRF element scanning

We first present μ-XRF mapping results because they are directly linked to our varve microfacies allowing us to precisely characterize the geochemical composition even for individual sublayers.

μ-XRF mapping. – The two epoxy-impregnated sediment blocks selected for μ-XRF element mapping allow direct comparison of the sediment composition with microfacies analyses. The calcite-organic and diatom-calcite varves of the Lateglacial and Early Holocene sediments from Lake Gościąż are best represented by the elements Ca (calcite), Si (diatoms and detrital matter) and Ti (detrital matter). However, XRF scanning does not provide elements associated with organic matter.

The mapping results are not quantified, but clearly reveal the main changes in relative amounts of the elements Ca, Si and Ti (Fig. 6). The stepwise transition from calcite-organic (subtype Ia) to diatom-calcite (type II) varves (in phases 1.1 to 1.4) at the onset of the YD is well reflected by the mapping results (Fig. 6B). Phase 1.1 (~12 705–12 630 cal. a BP) is dominated by Ca layers, while Ti and Si are only scarce, which agrees with a diatom-free varve microfacies. A slight increase in the log (Si/Ca) record at ~12 630 cal. a BP indicates a relative decrease of calcite at the boundary of phases 1.1 and 1.2. Phase 1.2 (~12 630–12 595 cal. a BP) shows slightly increasing amounts of Si and Ti. The beginning of phase 1.3 at ~12 595 cal. a BP reveals increasing amounts of Si and Ti, while the relative amount of Ca remains constant. Simultaneously, as shown by our microfacies, deposition of diatom sublayers commences and keeps rising, while the increase of quartz grains is only minor in phase 1.3. Hence, the increase of Si and of the log(Si/Ca) record in phase 1.3 mainly reflects a rise in diatoms, while the unvaried log(Si/Ti) ratio represents the concurrent rise in detrital matter. Conditions stabilize again at the boundary between phases 1.3 and 1.4 (at ~12 560 cal. a BP) as indicated by the more or less constant values of the log(Si/Ca) record in phase 1.4 (~12 560–12 530 cal. a BP). This phase is characterized by relatively high amounts of Si and Ti reflecting diatom sublayers and some finely dispersed detrital matter (Fig. 6B).

The YD/PB transition reflects a stepwise shift from diatom-calcite (varve type II) to calcite-organic (subtype Ib) varves (in phases 2.1 to 2.3) that is predominantly indicated by a decrease of diatoms (Fig. 6A). In addition, the Ti record reveals that detrital matter is generally low during this interval from ~11 555 to 11 435 cal. a BP. The diatom-dominated phase 2.1 (~11 555–11 525 cal. a BP) is characterized by well-pronounced diatom sublayers with occasional calcite sublayers resulting in highly variable log(Si/Ca) and log(Si/Ti) records. The boundary between phase 2.1 and 2.2 is marked by a relative increase in Ca, which is indicated by a decrease in the log(Si/Ca) record (Fig. 6A). The deposition of
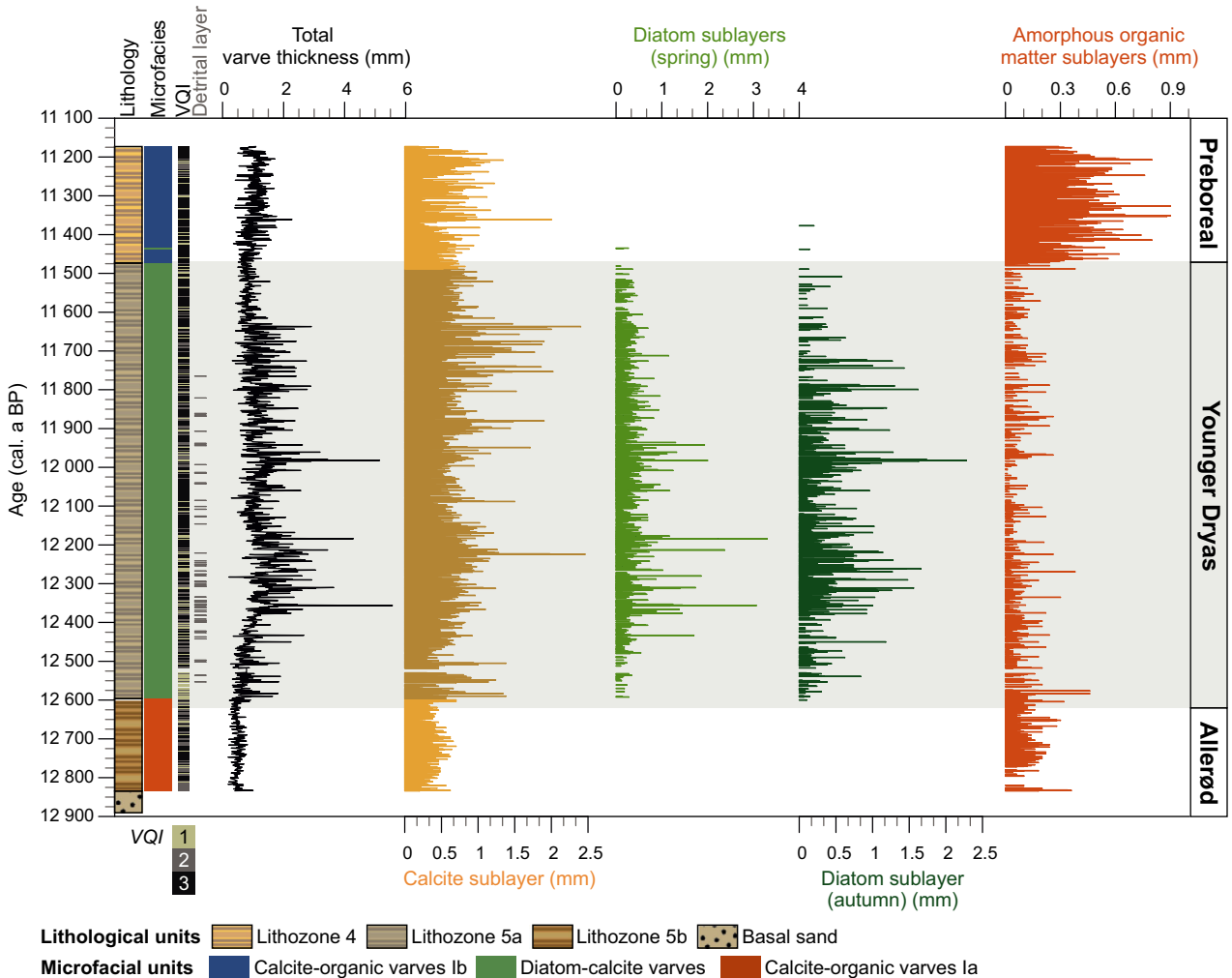
Fig. 4. Lithology, microfacies types, total varve thickness, thickness of selected sublayers, as well as occurrence of detrital sublayers. For diatom-calcite varves: the two diatom-bearing sublayers during spring (SL2 and SL3) are summarized (light green) and autumn diatoms represent SL5. The summer calcite sublayer is differentiated into (i) precipitated calcite with no diatom frustules (light yellow) and (ii) mainly re-suspended calcite with littoral diatom frustules (dark yellow). VQI = varve quality index.

diatom sublayers clearly declines at ~11 490 cal. a BP, which is reflected by a slight decrease in the log(Si/Ca) ratios. However, the boundary of phases 2.2 and 2.3 occurs only at ~11 470 cal. a BP and is marked by a sharp shift from relatively thin to thick amorphous organic matter sublayers. Diatoms and detrital matter (quartz) are absent in phase 2.3 and the origin of Si in this phase is not clear. However, the occurrence of Si in amorphous organic matter sublayers might suggest diatom dissolution in this phase.

XRF core scanning. – The two dominant varve types are diatom-calcite and calcite-organic varves that are best represented by log(Si/Ti), log(Si/Ca) and log(Ca/Ti) records (Figs 7, S3). Although detrital matter only occurs in very low amounts, the element Ti seems to play an important role in compositional variations.

In the log(Si/Ti) record (Fig. 7) distinct variations are absent and values remain relatively stable from the base of the studied interval, but increase slightly and fluctuate much more strongly between ~12 540 and ~11 625 cal. a BP. The interval of slightly higher fluctuation coincides with the frequent occurrence of thick diatom sublayers (Fig. 4). Also, the decline of the log(Si/Ti) record between ~11 700 and 11 470 cal. a BP corresponds to the decline of diatom sublayers (Figs 4, 7). The early PB is marked in the log(Si/Ti) record by an increase, although discrete diatom sublayers are not observed.

Similar to the log(Si/Ti) ratio, the log(Si/Ca) ratio is steady at the base of the studied interval, until it rises gradually from ~12 690 to 12 540 cal. a BP, covering the abrupt transition from calcite-organic (subtype Ia) varves to diatom-calcite (type II) varves (Fig. 7). After 12 540 cal. a BP the log(Si/Ca) ratio is generally elevated

Preboreal
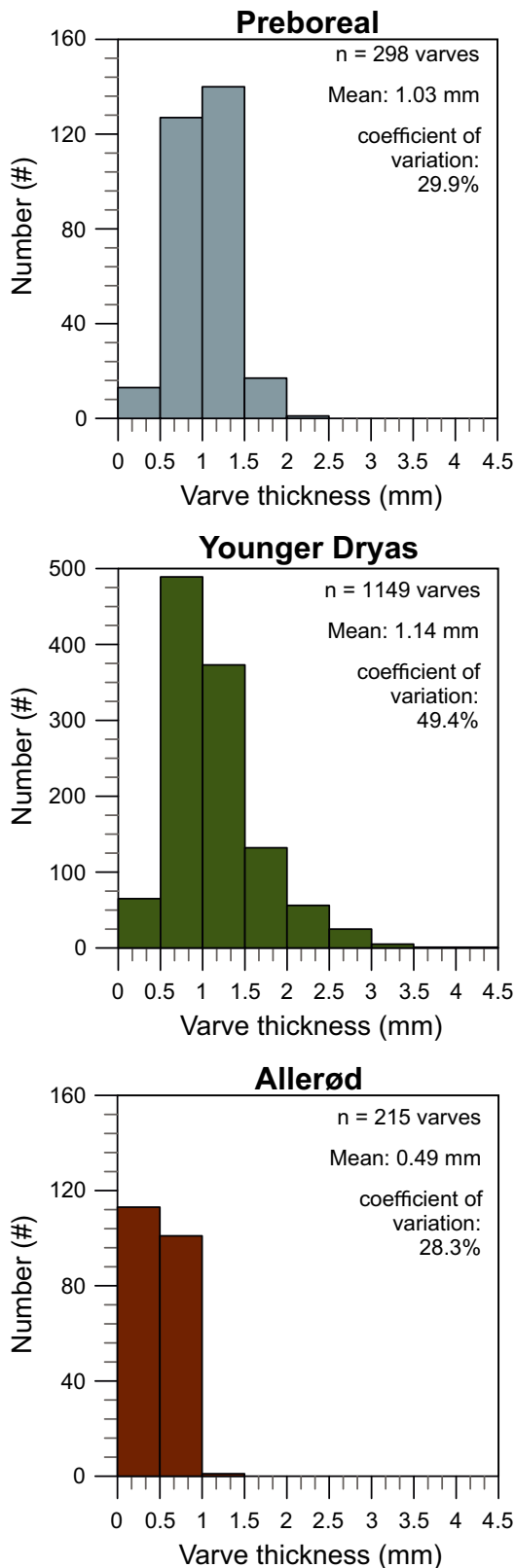

Younger Dryas

Allerød

Fig. 5. Frequency distribution plot of varve thicknesses for the late Allerød, Younger Dryas and early Preboreal. Number of varves (n), mean varve thickness (Mean) and coefficient of variation for each period are shown in the upper right corner.

(coinciding with the frequent occurrence of thick diatom sublayers), but decreases slightly until the YD/PB boundary, which is marked by one negative oscillation coinciding with the abrupt transition from diatom-calcite to calcite-organic (subtype Ib) varves. The early PB shows a continued steady decrease.

The log(Ca/Ti) record shows low variability at the base of the studied interval, but decreases gradually between ~12 690 and 12 540 cal. a BP (Fig. 7). This decrease coincides with the transition from calcite-organic (subtype Ia) varves to diatom-calcite varves, but is not as abrupt as observed in the microfacies (Fig. 7). After 12 540 cal. a BP, the log(Ca/Ti) record reveals a steady increase until the YD/PB boundary, which is interrupted by distinct fluctuations around the abrupt transition from diatom-calcite to calcite-organic (subtype Ib) varves. The early PB is marked by large-scale fluctuations.

Chironomid analyses

The detrended correspondence analysis (DCA) conducted for chironomid assemblages from the Gościąż sediments reveals a similar trend to MJAT estimations from the EE TS and SNP TS reconstructions (Fig. S4), indicating that summer temperature was the main driver of the midge communities during the study interval. Temporal resolution of the reconstructions depended on the availability of head capsules (hc) and ranges between 3 and 68 varves per sample (mean of 17 varves per sample) with lower resolution for samples that had to be merged due to too low hc numbers.

The reconstructions based on two different training sets generally show the same trends and changes (Figs 8, S4). However, the amplitudes of changes based on the SNP TS are significantly larger than those based on the EE TS, probably due to the larger temperature range covered by the SNP TS calibration data. The SNP TS includes temperatures down to 3.5 °C, while the EE TS does not include temperatures below 11.3 °C. Reconstructions with the SNP TS generally reveal lower MJAT, which is even more pronounced for the colder YD than for the warmer AL and PB (Fig. 8). This is most obvious for the minimum temperatures during the early YD (~12 620–11 950 cal. a BP), which reveal 2.8 °C colder reconstructions using the SNP TS (12.0 °C) compared to the EE TS (14.8 °C). In contrast, reconstructions of the warmest temperatures during the early PB (11 470–11 170 cal. a BP) differ only by 0.7 °C (SNP TS: 17.7 °C; EE TS: 18.4 °C). After relatively warm mean Allerød MJAT of 16.1 °C (SNP TS) and 16.9 °C (EE TS), both reconstructions exhibit a distinct gradual temperature decline of ~5 °C in SNP TS and ~2.5 °C in EE TS commencing at ~12 725 cal. a BP and lasting for ~140–180 years. Mean MJAT for the YD are ~14 °C (SNP TS) and ~16.5 °C (EE TS), but temperatures before
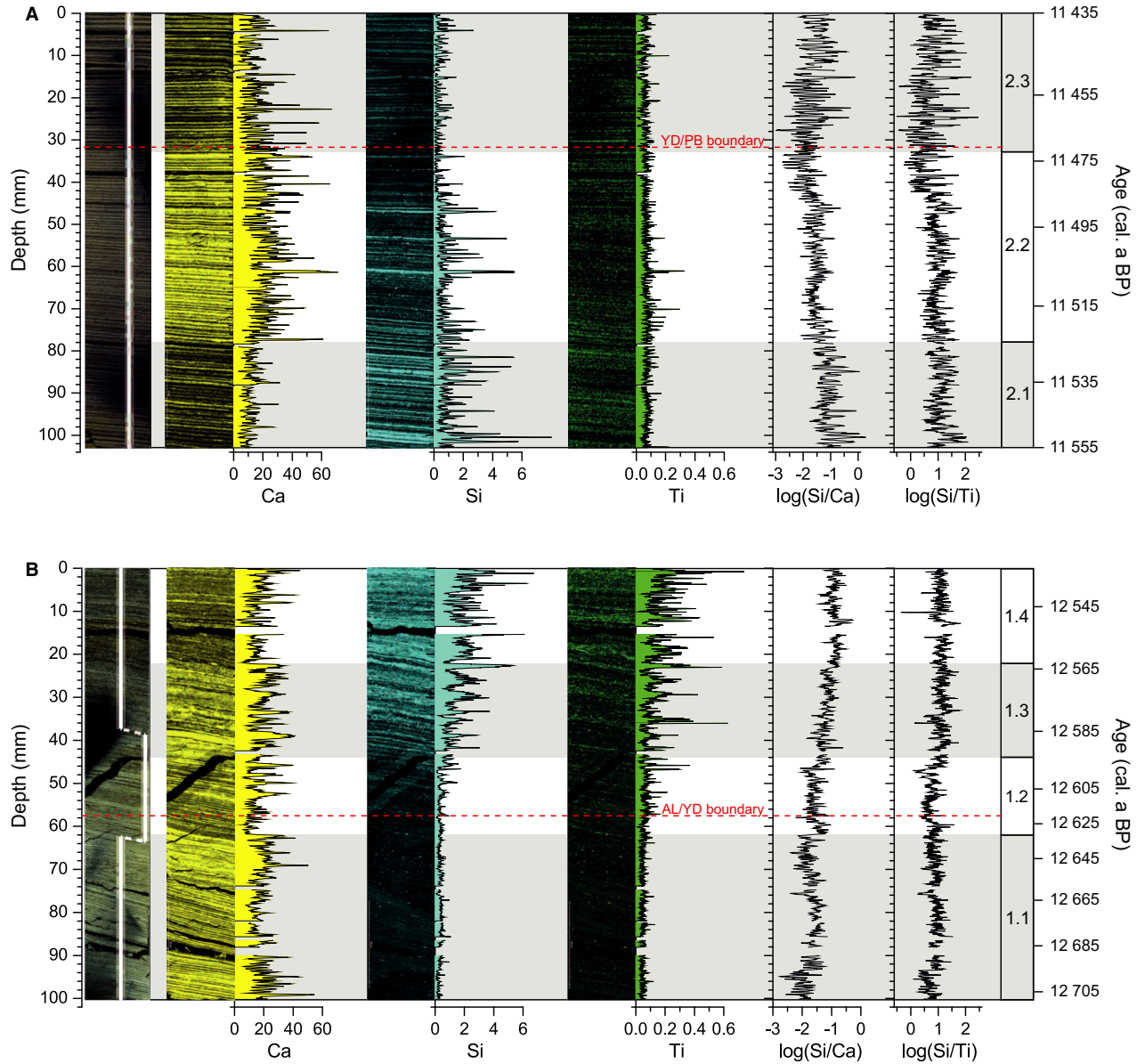
Fig. 6. Phases during YD transitions defined by μ-XRF mapping data. XRF counts and log-ratios are directly derived from μ-XRF mapping. From left to right: (i) thin section pictures with pathway of XRF scanning, (ii) maps of Ca (yellow), Si (blue) and Ti (green) with associated relative amounts (% counts), (iii) log-ratios of Si/Ca and Si/Ti. Dashed red lines mark the respective YD boundaries defined by our $\delta^{18}O_{carb}$ record. A. Sample GOS15-B8_153-163 cm: YD/PB transition. B. Sample GOS18-H5-1_42-52 cm: AL/YD transition.

~11 950 cal. a BP appear to be slightly colder (SNP TS mean: 13.6 °C; EE TS mean: 16.1 °C) than in the later part until ~11 470 cal. a BP (SNP TS mean: 14.7 °C; EE TS mean: 17.0 °C). The main temperature rise at the Holocene onset of 2.1 °C (EE TS) or 4.1 °C (SNP TS) occurred very rapidly in 40 and 60 years, respectively. Interestingly, directly before the onset of this increase a brief ~35 (SNP TS) to 50 (EE TS) year-long cold oscillation appears in both reconstructions. In the first century of the Holocene, MJAT reach highest values of the entire study interval before temperatures

slightly decline again (SNP TS mean: 16.6 °C; EE TS mean: 17.8 °C).

According to the EE TS reconstruction, 20 out of 95 samples remain below the 5% percentile threshold (minDC < 8.5053) and represent samples with good modern analogues. 42 samples have values over the 10% percentile threshold (minDC > 9.7531) and represent samples with poor modern analogues. According to the SNP TS reconstruction, 53 out of 95 samples remain below the 5% percentile threshold (minDC < 8.5775) and represent samples with good modern analogues. Five
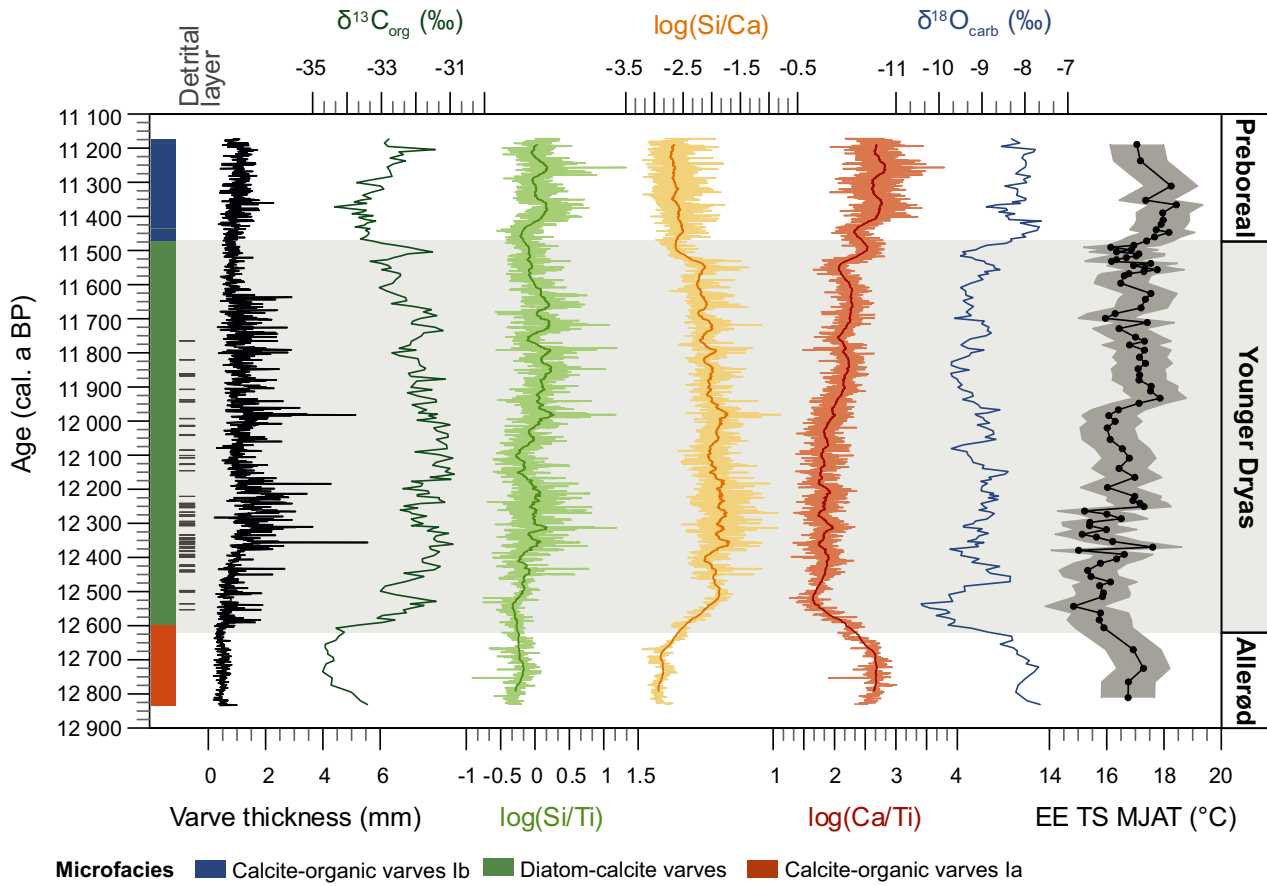
Fig. 7. Comparison of microfacies data (varve types, detrital layer occurrence, varve thickness) with continuous log(Si/Ti), log(Si/Ca) and log(Ca/Ti) records, as well as high-resolution stable isotope ($\delta^{13}C_{org}$, $\delta^{18}O_{carb}$) and chironomid-inferred mean July air temperature (MJAT) data for the Eastern European data training set (EE TS) (shaded background shows the standard error of prediction using bootstrapping cross-validation).

samples have values over the 10% percentile threshold (minDC > 10.0563) and represent samples with poor modern analogues.

Stable isotopes

The temporal resolution of the $\delta^{18}O_{carb}$ and $\delta^{13}C_{org}$ bulk sediment record is derived from contiguous 0.5–1 cm samples and varies between *c.* 4–14 varves cm^{-1} in the intervals from 11 350–11 170 and 12 520–11 580 cal. a BP, ~18–23 varves cm^{-1} in the interval 12 835–12 725 cal. a BP and ~8–24 varves cm^{-1} in the intervals from 11 580–11 350 and 12 725–12 525 cal. a BP.

$\delta^{18}O_{carb}$. – $\delta^{18}O_{carb}$ values are isotopically heavier during the late Allerød and Early Holocene with a maximum of $-7.62‰$ in the Early Holocene and lighter between -8.31 and $-10.42‰$ during the YD (Figs 7, 8). The $\delta^{18}O_{carb}$ decline of ~2.7‰ at the transition to the YD occurred in two steps between ~12 720 to 12 535 cal. a BP (185 years). Values increased again after an early YD

minimum. Within most of the YD, $\delta^{18}O_{carb}$ values fluctuate around 1‰, but do not show distinct trends. At the transition to the Holocene values rapidly increase by ~1.8‰ within ~75 years (11 505–11 430 cal. a BP). Directly before this transition, a 50-year oscillation with 0.9‰ more negative values occurred. During the first ~80 years of the Holocene values reached a maximum, which was followed by a brief (~50 years) negative oscillation at about 11 400 cal. a BP. From the declining/rising values at the YD transitions, we calculate ~5–7 °C colder annual air temperatures for the YD in agreement with published data (Goslar *et al.* 1998b). We point out the striking agreement with the $\delta^{18}O_{carb}$ record in previous studies (Kuc *et al.* 1998; Fig. 2B). This very good replicability, the shape of the curves and the measured absolute values confirm that the $\delta^{18}O_{carb}$ record is representative for Lake Gościąż and not influenced by local effects.

$\delta^{13}C_{org}$. – $\delta^{13}C_{org}$ values are isotopically lighter during the late Allerød and Early Holocene with a minimum of
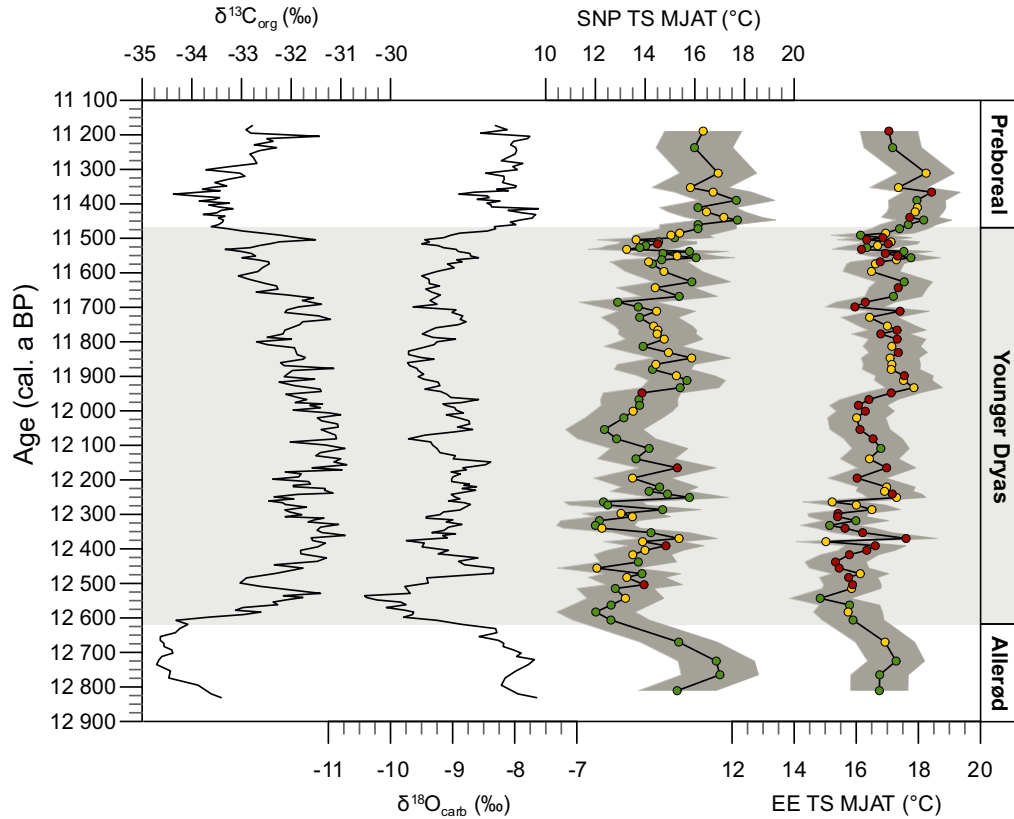
Fig. 8. Stable isotope data and chironomid-inferred mean July air temperature (MJAT) reconstructions using the Swiss-Norwegian-Polish Training Set (SNP TS) (Kotrys *et al.* 2020) and the East European Training Set (EE TS) (Luoto *et al.* 2019). Shaded background of temperature reconstructions shows the standard error of prediction using bootstrapping cross-validation. Statistic basis quality of the temperature reconstructions is represented by green (good), yellow (average) and red (poor) dots.

−34.7‰ in the late Allerød and heavier during the YD with a maximum of −30.9‰ (Figs 7, 8). A rapid increase of ~3‰ at the AL/YD transition occurred within ~80 years from ~12 610–12 530 cal. a BP. Values fluctuate around 1‰ during the early YD (~12 620–12 000 cal. a BP), before they slightly decrease during the late YD until ~11 470 cal. a BP. During the transition to the Holocene, the values rapidly drop by ~2‰ within ~40 years (11 505–11 465 cal. a BP) and after light values during the first ~150 years of the PB start to rise again. Directly before the major drop at the Holocene onset $\delta^{13}C_{org}$ values show a short (~30-year-long) oscillation to heavier values.

Discussion

The last deglaciation in the Northern Hemisphere is characterized by several short cold setbacks of which the YD was the last and most pronounced one. Cooling during the YD mainly affected the winter season and for central Poland January temperatures of about −20 °C are assumed (Isarin *et al.* 1998), resulting in a more pronounced seasonality of the climate (Denton *et al.* 2005). This was recently supported by a model study

suggesting mild but short YD summers (Schenk *et al.* 2018).

Younger Dryas definition and chronology

We define the YD in our new record in the same way as previous studies as the midpoint of the major shifts in $\delta^{18}O$ of bulk carbonate (Ralska-Jasiewiczowa *et al.* 1992; Kuc *et al.* 1998), which occurred nearly contemporaneously with vegetation changes (Goslar *et al.* 1993, 1998a; Kuc *et al.* 1998; Ralska-Jasiewiczowa *et al.* 1998a, 2003). Since our $\delta^{18}O_{carb}$ record resembles the previous record to a high degree (Fig. 2B), we are confident in adopting this YD boundary definition for further discussion. According to our independently established chronology, the AL/YD boundary is dated at 12 620+133/–231 cal. a BP and the YD/PB boundary at 11 470+126/–206 cal. a BP. The relatively large age uncertainties are mainly caused by anchoring the floating varve chronology through radiocarbon dating and age modelling (Bonk *et al.* 2021) and are considered as conservative estimates. Due to the excellent varve preservation with a mean VQI of 2.6, the counting uncertainty for the YD is low and we report

a YD duration of 1149+14/–22 varve years, which is in good agreement with previous varve counts of 1140±40 (Goslar *et al.* 1993, 1998a). The absolute ages for the YD boundaries in our chronology also agree within uncertainties with published dates for the Gościąż record (AL/YD boundary: 12 650±60 cal. a BP; 12 580±140 cal. a BP; YD/PB boundary: 11 510±40 cal. a BP; 11 440±120 cal. a BP; Goslar *et al.* 1998a, 1999). Furthermore, these ages are in agreement with the Meerfelder Maar (MFM) chronology (AL/YD boundary: 12 680±40 cal. a BP; YD/PB boundary: 11 590±40 cal. a BP; Brauer *et al.* 1999) and support that the YD in central Europe began later than Greenland Stadial 1 (GS-1) in NGRIP (12 846±138 to 11 653±99 cal. a BP; Rasmussen *et al.* 2006) due to time-transgressive cooling between Greenland and Europe (Rach *et al.* 2014).

Proxy interpretation

For the discussion of lake response to climate change we distinguish temperature and environmental proxies. The $\delta^{18}O_{carb}$ signal is interpreted as an annual temperature proxy controlled by the isotopic composition of precipitation and local air temperature (Leng 2006). Chironomid-inferred reconstructions represent MJAT.

$\delta^{13}C_{org}$ is interpreted as a proxy primarily for lake productivity (e.g. Lücke *et al.* 2003). Microscopic analyses reveal that calcite occurs either as endogenic calcite precipitated in the water column or in patches of re-suspended littoral calcite. This differentiation allows us to distinguish between sedimentation processes and, consequently, environmental conditions. Endogenic calcite precipitation in spring and summer is primarily controlled by temperature and lake productivity (Kelts & Hsü 1978), whereas deposition of re-suspended calcite, together with littoral diatoms, indicates higher lake water circulation and wave activity. Presence and thickness of amorphous organic sublayers are interpreted as a proxy for organic matter preservation in relation to seasonal anoxic conditions. Presence and thickness of diatom sublayers are applied as a proxy for lake productivity.

From (μ-)XRF scanning and mapping we selected Ca, Si and Ti as environmental proxies. Ca reflects calcite without distinction between endogenic and re-suspended calcite. Si is a proxy for both diatom frustules and detrital input (quartz, clay minerals), while Ti is not produced in the water column and thus unambiguously reflects detrital matter input. Since Ca and Si reflect different materials we apply various element ratios for a better distinction of sediment components. Log(Ca/Ti) ratios reflect relative variations of calcite and detrital matter, while log (Si/Ca) ratios show variations of diatoms/detrital matter and calcite. Log(Si/Ti) ratios reflect relative variations of diatoms and detrital matter and can be used as an indicator of diatom productivity.

Overall climate and environmental conditions

First, we discuss the general climatic states and environmental conditions during the study interval comprising the late Allerød (AL), the Younger Dryas (YD) and the early Preboreal (PB). In the second part of the discussion we will focus especially on the dynamic changes during the transitions into and out of the YD.

Late Allerød. – Chironomid and $\delta^{18}O_{carb}$ data show generally warm conditions during the late Allerød. Chironomid-based reconstructions from both training data sets (SNP TS and EE TS; Fig. 8) do not significantly differ and reveal July temperatures around 16–17 °C, which agrees well with previous July temperature reconstructions of 13–16 °C from pollen and plant macrofossils (Goslar *et al.* 1998b; Ralska-Jasiewiczowa *et al.* 1998a) and is only slightly lower than the recent July temperature of 18 °C (Wójcik & Przybylak 1998; Rozanski *et al.* 2010). The sedimentation during this period is characterized by a simple varve structure comprising an endogenic calcite sublayer with relatively large (~10–20 μm) idiomorphic calcite crystals and an amorphous organic matter sublayer (Fig. 3). The observed varve structure indicates a calm and stable lake environment with predominantly anoxic lake conditions (Brauer 2004). Weak lake water mixing is further suggested by the absence of discrete re-suspension sublayers. Catchment erosion was extremely low or even absent as indicated by the almost complete lack of detrital input from the catchment. Despite the warm summer temperatures aquatic bioproductivity was low as inferred from the absence of discrete diatom sublayers (Fig. 4), low log(Si/Ti) and log(Si/Ca) ratios, as well as low $\delta^{13}C_{org}$ values (Fig. 7), probably due to limited nutrient availability. Low productivity and catchment runoff are reflected in a mean varve thickness of only 0.49 mm, which is the lowest of the entire study interval. The low interannual variability of varve thickness (Fig. 5) and varve facies suggests that calm and stable lake conditions with a lack of extremes lasted for at least two centuries starting from the onset of varved lake gyttja formation. Similarly stable lake environment conditions during the late Allerød have been also reported from other lake records in Poland (Słowiński *et al.* 2017) and from Lake Meerfelder Maar (MFM) in Germany (Brauer *et al.* 1999; Lücke & Brauer 2004). The striking similarity of depositional processes in these lakes despite different basin morphology and catchment geology suggests a common, probably climatic, trigger.

Younger Dryas. – Cold conditions during the YD have been reported from many lake and speleothem records in Europe (von Grafenstein *et al.* 1999; Schwander *et al.* 2000; Frisia *et al.* 2005; Lauterbach *et al.* 2011; van Raden *et al.* 2013; Bartolomé *et al.* 2015), including Lake Gościąż (Kuc *et al.* 1998). From the Gościąż $\delta^{18}O_{carb}$

record a temperature decline of about 5 °C for the YD has been calculated (Goslar *et al.* 1998b). Our $\delta^{18}O_{carb}$ data closely resemble these published data (Fig. 2B), corroborating them as representative for the Lake Gościąż sediments. Recent studies report a strong seasonality of the YD climate with extremely low temperatures mainly in winter (Isarin *et al.* 1998), but relatively warm and short summers (Björck *et al.* 2002; Lücke & Brauer 2004; Birks & Birks 2014; Pawłowski *et al.* 2015; Schenk *et al.* 2018). YD summer temperature reconstructions of 14–16 °C for southern Scandinavia (Schenk *et al.* 2020) agree with our MJAT reconstructions ranging between 14 °C (SNP TS) and 16.5 °C (EE TS), depending on the calibration data applied (Fig. 8). These values are slightly higher than mean July temperatures of 10–13 °C derived from pollen and plant macrofossil reconstructions for Lake Gościąż (Goslar *et al.* 1998b). This difference might be explained by a bias due to the decreased length of the growing season.

The YD sediments generally are characterized by a complex varve structure with up to six sublayers (Fig. 3) including (i) discrete diatom sublayers, (ii) re-suspension sublayers composed of re-suspended calcite and littoral diatoms, and (iii) occasional up to ~0.6-mm-thick sublayers enriched in minerogenic detrital matter (mainly quartz) (Figs 4, 7). The regular occurrence of up to ~3-mm-thick planktonic diatom sublayers (Fig. 4) is also reflected in increased log(Si/Ca) and log(Si/Ti) ratios, indicating an enhanced lake productivity as supported by isotopically heavier $\delta^{13}C_{org}$ values (Fig. 7). The increased productivity can be explained by nutrient mobilization from the sediments due to intensive water circulation and nutrient input from the catchment. Strong water circulation and wave activity is supported by pronounced lake-internal sediment re-suspension. The intensified water circulation also led to better oxygenated conditions in the hypolimnion, which in turn caused organic matter degradation indicated by the distinct decline of organic matter sublayers. Slightly enhanced catchment erosion is inferred from the lower log(Ca/Ti) ratio and the occurrence of in total 62 sublayers enriched in silt-sized quartz. In addition to the generally dynamic internal lake processes and catchment erosion, the YD sedimentation is characterized by a pronounced interannual variability as inferred from the high variance of varve thickness (Fig. 5) and sublayer succession (Fig. 4).

Similarly unstable and dynamic sedimentation during the YD has been also reported from other lake records, for example MFM (Brauer *et al.* 1999, 2008; Lücke & Brauer 2004). However, we do not observe a distinct increase in detrital sediment input as in MFM, Kråkenes and Soppensee (Lotter 1991; Brauer *et al.* 1999; Bakke *et al.* 2009) that was also reported from Lake Gościąż (Goslar 1998). From the obvious but slight increase in detrital matter in our record we infer only moderate catchment erosion during the YD that resembles condi-

tions reported from the Rehwiese palaeolake (Neugebauer *et al.* 2012).

Environmental conditions were not uniform and gradual proxy changes during the YD suggest a general trend towards warmer and more stable conditions. Chironomid-based MJAT reconstructions reveal approximately 1 °C warmer summer temperatures after ~12 000 cal. a BP (Figs 7, 8), which is also reflected in the gradually increasing log(Ca/Ti) and decreasing log(Si/Ca) ratios, indicating an intensification in calcite precipitation. A gradual environmental response to warming is expressed by decreasing $\delta^{13}C_{org}$ values and diminution in diatom sublayer occurrence and thickness (Figs 4, 7), indicating decreasing productivity, probably caused by lower nutrient availability due to less intense lake water circulation. The increasing log(Ca/Ti) curve and the decline of detrital sublayers suggests an attenuation in catchment erosion likely due to soil stabilization in the catchment due to reforestation (Ralska-Jasiewiczowa *et al.* 1998a). Despite the obvious changes during the YD, we hesitate to state a YD bi-partition in Poland as has been earlier proposed (Goslar *et al.* 1998b; Pawłowski *et al.* 2015), because these changes are far more gradual than in western European sites located closer to the North Atlantic, which exhibit a distinct bi-partition of the YD (Brauer *et al.* 1999; Magny *et al.* 2001; Bakke *et al.* 2009).

Early Preboreal. – Our study interval includes the first ~300 years of the Preboreal. Chironomid-based MJAT reconstructions between 16.6 °C (SNP TS) and 17.8 °C (EE TS) are slightly higher than in the Allerød (Fig. 8), in agreement with July temperature reconstructions of about ~16 °C from pollen and plant macrofossils (Goslar *et al.* 1998b; Ralska-Jasiewiczowa *et al.* 1998a) and close to recent July temperatures (Wójcik & Przybylak 1998; Rozanski *et al.* 2010). The $\delta^{18}O_{carb}$ data show, after a short maximum, a ~50-year decline of ~1‰ around 11 400 cal. a BP, which might reflect a brief cold oscillation reported from the Greenland ice-cores (Rasmussen *et al.* 2007, 2014) and/or the Preboreal Oscillation (Björck *et al.* 1996). Sedimentation during the early PB is characterized by the recurrence of a simple varve structure, primarily consisting of an endogenic calcite and pronounced amorphous organic matter sublayer (Fig. 4), similar to those formed in the late Allerød. The main difference compared to the late Allerød varves are thicker amorphous organic matter sublayers, which often also include scattered calcite and vivianite. This suggests better organic matter preservation due to anoxic conditions, likely favoured by increased inflow of mineral-rich groundwater after permafrost thawing during the Early Holocene (Starkel *et al.* 1998; Błaszkiewicz 2011) and more efficient lake sheltering due to catchment reforestation (Ralska-Jasiewiczowa *et al.* 1998d; Dräger *et al.* 2017; Żarczyński *et al.* 2019). The absence of diatom sublayers and lighter

$\delta^{13}C_{org}$ values (Figs 4, 7) suggest low lacustrine productivity. However, we cannot exclude growth of other algae species like, for example, green algae that do not leave visible remains in the sediments (Marciniak & Szeroczyńska 1998; Ralska-Jasiewiczowa *et al.* 1998a) and might explain an increase in productivity suggested by the rise in $\delta^{13}C_{org}$ values. The lack of discrete diatom sublayers might be also explained by dissolution of diatom frustules as suggested by amorphous organic matter sublayers enriched in silicon (Figs 6, 9). The further decline of already weak catchment erosion, indicated by high log(Ca/Ti) ratios, reflects the full Holocene forest recovery (Ralska-Jasiewiczowa *et al.* 1998d). In contrast to the YD, the interannual variability in varve thickness (Fig. 5) and composition was low, indicating stable environmental conditions.

Lake responses into and out of the Younger Dryas

Due to their seasonal time resolution, varved sediments are ideal to investigate processes and times of lake responses to rapid climate shifts in the past. Previous studies focusing on vegetation changes at the YD/PB transition have established the Lake Gościąż sediments as particularly suitable for such high-resolution studies (Ralska-Jasiewiczowa *et al.* 2003). Here, we extend these investigations with a focus on novel sedimentological and geochemical proxies and compare periods of rapid warming (YD/PB transition) with periods of rapid cooling (AL/YD transition). For this purpose and in addition to classical XRF element scanning and microfacies analyses, we apply high-resolution μ-XRF element mapping for a ~120-year (YD/PB) and a ~175-year (AL/YD) time window covering the transitions into and out of the YD (Fig. 9).

AL/YD transition. – Both chironomid- and $\delta^{18}O_{carb}$-based reconstructions show gradually declining air temperatures for about 140 (SNP TS) to 180 years (EE TS and $\delta^{18}O_{carb}$) starting at ~12 720 cal. a BP (Fig. 8). The duration of the main decline period is about the same as reported from biomarker isotope reconstructions from MFM (Rach *et al.* 2014). The resolution of chironomid-based reconstructions for this transition is rather low due to the scarcity of head capsules. In the higher resolved $\delta^{18}O_{carb}$ data a clear two-step decline in air temperature appears, which was moderate before ~12 630 cal. a BP and stronger afterwards (Figs 7, 8, 9).

Lake responses to the temperature lowering occurred as a succession in four phases (1.1–1.4 in Fig. 9). During the slow temperature decline in the initial phase 1.1 (~12 720–12 630 cal. a BP), seasonal sublayer composition and element data do not show distinct changes. Phase 1.2 from ~12 630–12 595 cal. a BP reflects a period of accelerated temperature decline and includes the onset of the YD at the midpoint of the $\delta^{18}O_{carb}$

decrease. During this phase, Si and Ti counts show a weak increase, while the log(Si/Ca) ratio is slightly higher, indicating a relative decrease in calcite due to slightly higher diatom productivity and catchment erosion. Higher lake productivity is supported by an increase of $\delta^{13}C_{org}$ values caused by enrichment of ^{13}C in the lake water due to higher photosynthesis (Leng 2006). The onset of phase 1.3 at ~12 595 cal. a BP marks a prominent and abrupt shift in the sedimentation regime due to a sudden increase in diatom productivity. This is expressed by the first occurrence of discrete diatom sublayers leading to an increase in varve thickness, an abrupt rise in the log(Si/Ca) record and in the substantially higher amounts of Si (Fig. 9). The abruptness of this shift suggests that a threshold in nutrient availability has been crossed, probably triggered by nutrient remobilization from the sediments due to intensified lake water circulation and by nutrient input from the catchment. Stronger water circulation also explains the concomitant occurrence of re-suspended calcite and littoral diatoms and likely led to an intensified ventilation of the lake bottom as reflected in the decrease of amorphous organic matter sublayers due to organic matter decomposition. Higher Ti amounts further indicate an increase in catchment erosion. During the final phase 1.4 (~12 560–12 530 cal. a BP) conditions stabilize as indicated by regular deposition of diatom sublayers, primarily constant log(Si/Ca) ratios and high amounts of Si (Fig. 9). High amounts of Ti and sporadic occurrence of thin discrete detrital sublayers since ~12 553 cal. a BP (Fig. 9) reflect finely dispersed detrital matter and small-scale erosion events.

The timing of lake sedimentation response to climate cooling differs between proxies. Main changes in proxies for calcite precipitation, lake productivity and catchment erosion occurred within ~100 years from ~12 630–12 530 cal. a BP during phases 1.2 to 1.4 (Fig. 9), broadly coinciding with the second, steeper decline in $\delta^{18}O_{carb}$. In contrast to the geochemical changes, the seasonal sedimentation pattern changed faster within ~35 years between ~12 595–12 560 cal. a BP, indicating that threshold processes are involved. This applies especially for the occurrence of discrete diatom sublayers, which suddenly appeared ~25 years after the midpoint of $\delta^{18}O_{carb}$ and ~125 years after $\delta^{18}O_{carb}$ started to decline. Similar environmental delays have been reported from MFM (Rach *et al.* 2014), suggesting a common driver rather than local effects. In both lakes, the sudden appearance of discrete diatom and re-suspension sublayers and the parallel decline in amorphous organic matter sublayers point to a pronounced sensitivity to intensified water circulation changes driven by winds (Brauer *et al.* 2008) and/or seasonality rather than to declining temperatures. Differences between the lakes appear in the intensity of catchment erosion at the YD onset. After the
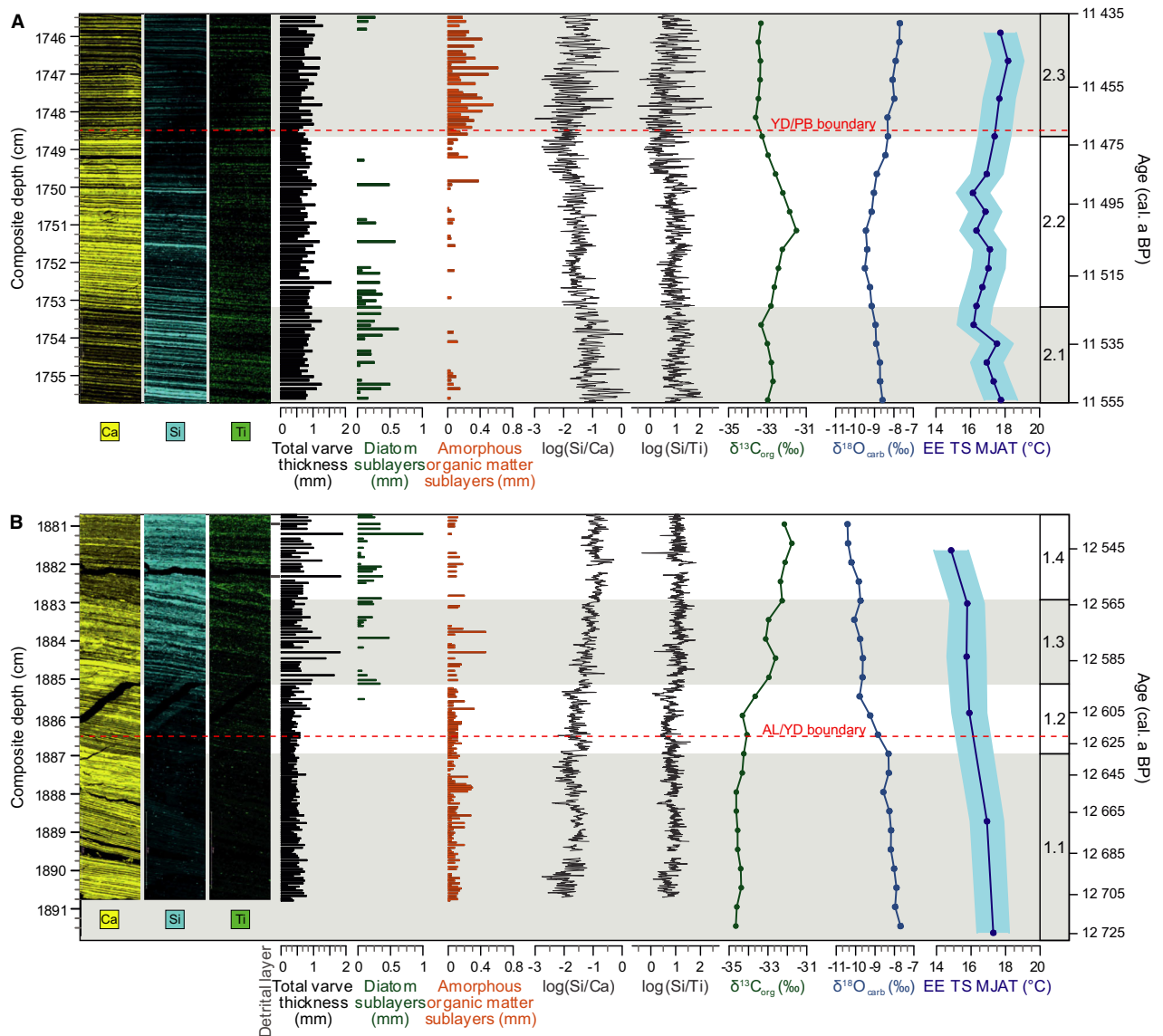
Fig. 9. Zoom in at the A. YD/PB transition (~120 years). B. AL/YD transition (~190 years). Left: µ-XRF mapping of Ca, Si and Ti. Right: selected microfacies data, XRF log-ratios of Si/Ca and Si/Ti, $\delta^{13}C_{org}$, $\delta^{18}O_{carb}$ and chironomid-inferred mean July air temperature (MJAT) for the Eastern European data training set (EE TS). All three diatom sublayers from varve type II (SL2, 3 and 5) are summarized. Dashed red lines mark the respective YD boundaries defined by our $\delta^{18}O_{carb}$ record.

almost complete lack of detrital matter in the late Allerød in both lake records, the increase in detrital material was far more moderate in Lake Gościąż (Brauer *et al.* 1999; Litt *et al.* 2001).

YD/PB transition. – From the 1.8‰ increase in $\delta^{18}O_{carb}$ within ~70 years at the YD/PB transition an annual air temperature rise of ~5 °C is inferred that agrees with previous results from Lake Gościąż (Fig. 2B; Goslar *et al.* 1998b). The abrupt warming within ~70 years is in agreement with reports from MFM (Rach *et al.* 2014). The temperature rise is clearly traced also in both chironomid-based reconstructions (Fig. 8). The larger

amplitude of the warming in the SNP TS (4.1 °C) compared to the EE TS (2.1 °C) reconstruction is due to the lower YD temperatures derived from the SNP TS data. In this respect, the EE TS reconstruction is in better agreement with model results suggesting warm YD summers (Schenk *et al.* 2018). The major air temperature rise at the Holocene onset was directly preceded by a ~50-year-long drop in $\delta^{18}O_{carb}$ of ~0.9‰, which has been earlier reported from Lake Gościąż and related to changes in seasonal precipitation (Ralska-Jasiewiczowa *et al.* 2003). Since this fluctuation also appears in our chironomid-based reconstructions we consider an air temperature drop as a more likely explanation. This short

cold episode might be related to a brief drop in North Atlantic sea surface temperatures (Bakke *et al.* 2009).

The main and rapid lake responses at the YD/PB transition in Lake Gościąż as shown in Fig. 9 were preceded by gradual environmental changes. About 465 years earlier at ~11 935 cal. a BP diatom sublayer frequency and thickness gradually declined (Fig. 4) and between ~11 700–11 630 cal. a BP further decreases in varve thickness, diatom sublayer thickness and occurrence (Fig. 4), as well as in log(Si/Ti) ratios and $\delta^{13}C_{org}$ values occurred (Fig. 7). All point to more frequent occurrence of years with weaker water circulation and limited nutrient remobilization from the bottom sediments. The absence of years with pronounced diatom blooms might be also related to blooms of green algae, like for example *Tetraedron* (Ralska-Jasiewiczowa *et al.* 2003). The attenuation of catchment erosion is reflected in the increase of the log(Ca/Ti) ratio since about 12 000 cal. a BP (Fig. 7) and the cessation of discrete detrital layer deposition at ~11 765 cal. a BP (Fig. 7), both reflecting a gradual recovery of forest vegetation and stabilization of slope processes (Ralska-Jasiewiczowa *et al.* 1998a).

The final transition from the YD into the Holocene occurred in three phases (2.1–2.3 in Fig. 9) of which the first phase 2.1 reflects the late YD environment with reduced varve thickness, diatom productivity and nearly absent detrital input. Phase 2.2 commenced abruptly at ~11 525 cal. a BP and appears particularly distinct in the element maps (Figs 6, 9). High relative amounts of Ca, the decreasing log(Si/Ca) ratio and thin section observations suggest intensified endogenic calcite precipitation. An intensified calcite formation during times of declining temperatures, as expressed in the anti-correlation of the log(Si/Ca) and $\delta^{18}O_{carb}$ curves, is unexpected since log(Si/Ca) generally parallels the temperature curves in all other parts of the study interval. This suggests other controls than temperature on calcite precipitation during this short period. A possible explanation might be higher concentrations of calcium and carbonate ions in the lake water either due to a brief lake level decline (Ralska-Jasiewiczowa *et al.* 2003) and/or higher groundwater inflow. At ~11 490 cal. a BP, log(Si/Ca) ratios decrease, reflecting the cessation of diatom deposition. The onset of phase 2.3 at ~11 470 cal. a BP is marked by an abrupt shift from one year to the next, when thick amorphous organic matter sublayers begin to regularly form in every year (Fig. 9). The abruptness of this shift suggests that a threshold for predominantly anoxic conditions at the lake bottom was crossed. This shift is very distinct in the element maps (Fig. 9) and the macroscopically visible colour change of the sediments from light to dark. Interestingly, this main shift in the depositional environment of the lake coincides with the midpoint of the temperature rise, which marks the defined onset of the Holocene (Fig. 7). Varve thickness does not change at that point, because calcite sublayer

thickness does not change and cessation of diatom sublayers is compensated by amorphous organic matter sublayers.

Comparison of the YD transitions. – The gradual cooling at the onset of the YD lasted for about one and a half centuries and thus 2–3 times longer than the warming at the Holocene onset, which in addition was preceded by a brief cold oscillation of about the same duration as the final temperature rise itself. The lake responses are complex and in general, geochemical proxies seem to respond more gradually, whereas seasonal sedimentation can change within a few years, suggesting that threshold effects are involved. Endogenic calcite formation as reflected in log(Ca/Ti) and log(Si/Ca) is the only parameter that mirrors temperature changes directly. Proxies reflecting lake productivity and organic matter preservation respond to lake-internal processes largely driven by water circulation, which is considered a major factor for lacustrine sedimentation. Detrital input as a proxy for erosion processes in the catchment is predominantly controlled by vegetation cover and thus only indirectly by climate change. The detrital portion in our study interval is generally low and shows only a slight increase/decrease at the onset/end of the YD, indicating that despite an obvious reduction in forest cover (Ralska-Jasiewiczowa *et al.* 1998a) the catchment remained largely vegetated even during the YD.

The main lake response to the cooling at the beginning of the YD was an increase in diatom productivity and lake-internal re-suspension processes accompanied by a decline in organic matter preservation. The shift in seasonal deposition commenced ~125 years after air temperature started to decline and occurred mainly during the second half of the period of cooling (Fig. 9). Interestingly, distinct environmental changes commenced ~90 years after onset of cooling at about the midpoint of the air temperature decline that is defined as the onset of the YD. A critical threshold was crossed about 35 years later at ~12 595 cal. a BP when the first discrete diatom blooms occurred. The delayed lake response to the cooling might be rather explained with a particular sensitivity to lake circulation than to temperature. One might speculate that major changes in atmospheric circulation, which ultimately triggered the changes in sedimentation, occurred with a delay of some decades after temperatures started to decline.

Lake responses to the rapid and major warming at the end of the YD occurred instantaneously. However, productivity and erosion proxies showed first signs of changes within the lake and catchment already a few centuries before the main warming (Figs 4, 7), probably reflecting an initial increase in MJAT, water circulation and catchment vegetation (Ralska-Jasiewiczowa *et al.* 1998a) in the late YD. During the brief cold oscillation before the final warming, mechanisms of lake responses changed and likely were controlled by local hydrology

rather than temperature. At the same time when temperature rise commenced at ~11 505 cal. a BP, the frequency of diatom blooms rapidly decreased further and ceased before the midpoint of the temperature rise. About 20 years later, regular deposition of thicker amorphous organic sublayers began (Fig. 9). This reflects the onset of the typical anoxic sedimentation pattern of the PB, even a few decades before the temperature rise came to an end. This immediate lake response suggests a pronounced sensitivity to climate warming compared to a larger resilience with respect to climate cooling.

Conclusions

Our results provide new insights into rapid climate change and lake system responses at the onset and demise of the YD. The chironomid-based MJAT reconstructions support the hypothesis from several studies that the summer temperature decline was less pronounced during the YD. Sedimentation during the YD still is predominantly controlled by lake-internal processes and the increase of catchment material is only weak to moderate in Lake Gościąż, which is uncommon but not unique. The seasonal sedimentation pattern of Lake Gościąż during the YD indicates a dynamic lake system, primarily controlled by intensified water circulation and wave activity. Furthermore, the YD in Lake Gościąż is characterized by a pronounced interannual variability suggesting unstable weather conditions.

In Lake Gościąż, the rapid transitions into and out of the YD exhibit distinct differences in both the temperature changes themselves and lake system responses provoked by these changes. The major warming at the end of the YD occurred in 40–70 years and thus faster than the cooling at the onset of the YD (140–180 years). The lake system was more resilient to the cooling at the YD onset and first changes in environmental proxies lagged the cooling by ~90 years. In contrast, lake responses to the terminal PB warming occurred instantaneously.

In general, different environmental proxies derived from microfacies, XRF element scanning and stable isotope analyses do not respond synchronously, but with small leads and lags. Element and stable isotope geochemistry commonly changes slightly more gradually, while seasonal sublayer formation tends to change abruptly within a few years suggesting that threshold processes are involved. Such potential differences in proxy responses to climate change should be considered for proxy-based synchronization of sediment records from different lakes.

References

Adrian, R., Hessen, D. O., Blenckner, T., Hillebrand, H., Hilt, S., Jeppesen, E., Livingstone, D. M. & Trolle, D. 2016: Environmental impacts—lake ecosystems. *In* Quante, M. & Colijn, F. (eds.): *North Sea Region Climate Change Assessment*, 315–340. Springer Nature, Berlin.

Adrian, R., O'Reilly, C. M., Zagarese, H., Baines, S. B., Hessen, D. O., Keller, W., Livingstone, D. M., Sommaruga, R., Straile, D., Van Donk, E., Weyhenmeyer, G. A. & Winder, M. 2009: Lakes as sentinels of climate change. *Limnology and Oceanography 54*, 2283–2297.

Bakke, J., Lie, Ø., Heegaard, E., Dokken, T., Haug, G. H., Birks, H. H., Dulski, P. & Nilsen, T. 2009: Rapid oceanic and atmospheric changes during the Younger Dryas cold period. *Nature Geoscience 2*, 202–205.

Bartolomé, M., Moreno, A., Sancho, C., Stoll, H. M., Cacho, I., Spötl, C., Belmonte, Á., Edwards, R. L., Cheng, H. & Hellstrom, J. C. 2015: Hydrological change in Southern Europe responding to increasing North Atlantic overturning during Greenland Stadial 1. *Proceedings of the National Academy of Sciences of the United States of America 112*, 6568–6572.

Birks, H. H. & Birks, H. J. B. 2014: To what extent did changes in July temperature influence Lateglacial vegetation patterns in NW Europe? *Quaternary Science Reviews 106*, 262–277.

Björck, S., Bennike, O., Rosén, P., Andresen, C. S., Bohncke, S., Kaas, E. & Conley, D. 2002: Anomalously mild Younger Dryas summer conditions in southern Greenland. *Geology 30*, 427–430.

Björck, S., Kromer, B., Johnsen, S., Bennike, O., Hammarlund, D., Lemdahl, G., Possnert, G., Rasmussen, T. L., Wohlfarth, B., Hammer, C. U. & Spurk, M. 1996: Synchronized terrestrial-

atmospheric deglacial records around the North Atlantic. *Science* 274, 1155–1160.

Błaszkiewicz, M. 2011: Timing of the final disappearance of permafrost in the central European Lowland, as reconstructed from the evolution of lakes in N Poland. *Geological Quarterly* 55, 361–374.

Błaszkiewicz, M., Piotrowski, J. A., Brauer, A., Gierszewski, P., Kordowski, J., Kramkowski, M., Lamparski, P., Lorenz, S., Noryśkiewicz, A. M., Ott, F., Słowiński, M. & Tyszkowski, S. 2015: Climatic and morphological controls on diachronous postglacial lake and river valley evolution in the area of Last Glaciation, northern Poland. *Quaternary Science Reviews* 109, 13–27.

Bonk, A., Müller, D., Ramisch, A., Kramkowski, M. A., Noryśkiewicz, A. M., Sekudewicz, I., Gąsiorowski, M., Luberda-Durnaś, K., Słowiński, M., Schwab, M., Tjallingii, R., Brauer, A. & Błaszkiewicz, M. 2021: Varve microfacies and chronology from a new sediment record of Lake Gościąż (Poland). *Quaternary Science Reviews* 251, 106715, https://doi.org/10.1016/j.quascirev.2020.106715.

Botta, F., Dahl-Jensen, D., Rahbek, C., Svensson, A. & Nogués-Bravo, D. 2019: Abrupt change in climate and biotic systems. *Current Biology* 29, R1045–R1054.

Brauer, A. 2004: Annually laminated lake sediments and their palaeoclimatic relevance. *In* Fischer, H., Kumke, T., Lohmann, G., Flöser, G., von Miller, H., Storch, H. & Negendank, J. F. W. (eds.): *The Climate in Historical Times. GKSS School of Environmental Research*, 109–127. Springer, Berlin.

Brauer, A. & Casanova, J. 2001: Chronology and depositional processes of the laminated sediment record from Lac d'Annecy, French Alps. *Journal of Paleolimnology* 25, 163–177.

Brauer, A., Endres, C., Günter, C., Litt, T., Stebich, M. & Negendank, J. F. W. 1999: High resolution sediment and vegetation responses to Younger Dryas climate change in varved lake sediments from Meerfelder Maar, Germany. *Quaternary Science Reviews* 18, 321–329.

Brauer, A., Haug, G. H., Dulski, P., Sigman, D. M. & Negendank, J. F. W. 2008: An abrupt wind shift in western Europe at the onset of the Younger Dryas cold period. *Nature Geoscience* 1, 520–523.

Clark, P. U., Shakun, J. D., Baker, P. A., Bartlein, P. J., Brewer, S., Brook, E., Carlson, A. E., Cheng, H., Kaufman, D. S., Lui, Z., Marchitto, T. M., Mix, A. C., Morrill, C., Otto-Bliesner, B. L., Pahnke, K., Russell, J. M., Whitlock, C., Adkins, J. F., Blois, J. L., Clark, J., Colman, S. M., Curry, W. B., Flower, B. P., He, F., Johnson, T. C., Lynch-Stieglitz, J., Markgraf, V., McManus, J., Mitrovica, J. X., Moreno, P. I. & Williams, J. W. 2012: Global climate evolution during the last deglaciation. *Proceedings of the National Academy of Sciences of the United States of America* 109, E1134–E1142.

Croudace, I. W., Rindby, A. & Rothwell, R. G. 2006: ITRAX: description and evaluation of a new multi-function X-ray core scanner. *In* Rothwell, R. G. (ed.): *New Techniques in Sediment Core Analysis*, 51–63. Geological Society, London, Special Publications 267.

Denton, G. H., Alley, R. B., Comer, G. C. & Broecker, W. S. 2005: The role of seasonality in abrupt climate change. *Quaternary Science Reviews* 24, 1159–1182.

Denton, G. H., Anderson, R. F., Toggweiler, J. R., Edwards, R. L., Schaefer, J. M. & Putnam, A. E. 2010: The Last Glacial Termination. *Science* 328, 1652–1656.

Dräger, N., Theuerkauf, M., Szeroczyńska, K., Wulf, S., Tjallingii, R., Plessen, B., Kienel, U. & Brauer, A. 2017: Varve microfacies and varve preservation record of climate change and human impact for the last 6000 years at Lake Tiefer See (NE Germany). *The Holocene* 27, 450–464.

Frisia, S., Borsato, A., Spötl, C., Villa, I. & Cucchi, F. 2005: Climate variability in the SE Alps of Italy over the past 17 000 years reconstructed from a stalagmite record. *Boreas* 34, 445–455.

Gierszewski, P. 1993: Chemical denudation within the drainage basin of the Ruda River in 1990 hydrological year. *Zeszyty Instytutu Geografii i Przestrzennego Zagospodarowania PAN* 12, 29–45. (in Polish with English summary).

Giziński, A., Kentzer, A., Mieszczankin, T., Żbikowski, J. & Żytkowicz, R. 1998: Hydrobiological characteristics and modern sedimentation of Lake Gościąż. *In* Ralska-Jasiewiczowa, M., Goslar, T., Madeyska, T. & Starkel, L. (eds.): *Lake Gościąż, Central Poland. A Monographic*

Study. Part 1, 49–61. W. Szafer Institute of Botany, Polish Academy of Sciences, Kraków.

Goslar, T. 1998: Record of laminae thickness of the Lake Gościąż sediments, and its correlation with absolutely dated tree-ring width sequences. *In* Ralska-Jasiewiczowa, M., Goslar, T., Madeyska, T. & Starkel, L. (eds.): *Lake Gościąż, Central Poland. A Monographic Study. Part 1*, 104–110. W. Szafer Institute of Botany, Polish Academy of Sciences, Kraków.

Goslar, T., Arnold, M., Bard, E., Kuc, T., Pazdur, M. F., Ralska-Jasiewiczowa, M., Różański, K., Tisnerat, N., Walanus, A., Wicik, B. & Więckowski, K. 1995: High concentration of atmospheric ¹⁴C during the Younger Dryas cold episode. *Nature* 377, 414–417.

Goslar, T., Arnold, M. & Pazdur, M. F. 1998a: Variations of atmospheric ¹⁴C concentrations at the Pleistocene/Holocene transition, reconstructed from the Lake Gościąż sediments. *In* Ralska-Jasiewiczowa, M., Goslar, T., Madeyska, T. & Starkel, L. (eds.): *Lake Gościąż, Central Poland. A Monographic Study. Part 1*, 162–171. W. Szafer Institute of Botany, Polish Academy of Sciences, Kraków.

Goslar, T., Kuc, T., Pazdur, M. F., Ralska-Jasiewiczowa, M., Różański, K., Szeroczyńska, K., Walanus, A., Wicik, B., Wieckowski, K., Arnold, M. & Bard, E. 1992: Possibilities for reconstructing radiocarbon level changes during the Late Glacial by using a laminated sequence of Gościąż Lake. *Radiocarbon* 34, 826–832.

Goslar, T., Kuc, T., Ralska-Jasiewiczowa, M., Różański, K., Arnold, M., Bard, E., van Geel, B., Pazdur, M. F., Szeroczyńska, K., Wicik, B., Więckowski, K. & Walanus, A. 1993: High-resolution lacustrine record of the Late Glacial/Holocene transition in Central Europe. *Quaternary Science Reviews* 12, 287–294.

Goslar, T., Pazdur, A., Pazdur, M. F. & Walanus, A. 1989: Radiocarbon and varve chronologies of annually laminated lake sediments of Gościąz Lake, Central Poland. *Radiocarbon* 31, 940–947.

Goslar, T., Ralska-Jasiewiczowa, M., Starkel, L., Demske, D., Kuc, T., Łącka, B., Szeroczyńska, K., Wicik, B. & Więckowski, K. 1998b: Discussion of the Late-Glacial recorded in the Lake Gościąż sediments. *In* Ralska-Jasiewiczowa, M., Goslar, T., Madeyska, T. & Starkel, L. (eds.): *Lake Gościąż, Central Poland. A Monographic Study. Part 1*, 171–175. W. Szafer Institute of Botany, Polish Academy of Sciences, Kraków.

Goslar, T., Wohlfarth, B., Björck, S., Possnert, G. & Björck, J. 1999: Variations of atmospheric ¹⁴C concentrations over the Allerød-Younger Dryas transition. *Climate Dynamics* 15, 29–42.

von Grafenstein, U., Erlenkeuser, H., Brauer, A., Jouzel, J. & Johnsen, S. J. 1999: A mid-European decadal isotope-climate record from 15,500 to 5000 years B.P. *Science* 284, 1654–1657.

Havens, K. & Jeppesen, E. 2018: Ecological responses of lakes to climate change. *Water* 10, 917, https://doi.org/10.3390/w10070917.

Isarin, R. F. B., Renssen, H. & Vandenberghe, J. 1998: The impact of the North Atlantic Ocean on the Younger Dryas climate in northwestern and central Europe. *Journal of Quaternary Science* 13, 447–453.

Juggins, S. 2007: *C2 Version 1.5 User Guide. Software for Ecological and Palaeoecological Data Analysis and Visualisation*. 73 pp. Newcastle University, Newcastle upon Tyne.

Kelts, K. & Hsü, K. J. 1978: Freshwater carbonate sedimentation. *In* Lerman, A. (ed.): *Lakes. Chemistry, Geology, Physics*, 295–323. Springer, New York.

Kępczyński, K. & Noryśkiewicz, A. 1998: Vegetation of the Gostynińskie Lake District. *In* Ralska-Jasiewiczowa, M., Goslar, T., Madeyska, T. & Starkel, L. (eds.): *Lake Gościąż, Central Poland. A Monographic Study. Part 1*, 29–33. W. Szafer Institute of Botany, Polish Academy of Sciences, Kraków.

Kotrys, B., Płóciennik, M., Sydor, P. & Brooks, S. J. 2020: Expanding the Swiss-Norwegian chironomid training set with Polish data. *Boreas* 49, 89–107.

Kruczkowska, B., Błaszkiewicz, M., Jonczak, J., Uzarowicz, Ł., Moska, P., Brauer, A., Bonk, A. & Słowiński, M. 2020: The Late Glacial pedogenesis interrupted by aeolian activity in Central Poland – records from the Lake Gościąż catchment. *Catena* 185, 104286, https://doi.org/10.1016/j.catena.2019.1042.

Kuc, T., Różański, K. & Duliński, M. 1998: Isotopic indicators of the Late-Glacial/Holocene transition recorded in the sediments of Lake

Gościąż. *In* Ralska-Jasiewiczowa, M., Goslar, T., Madeyska, T. & Starkel, L. (eds.): *Lake Gościąż, Central Poland. A Monographic Study. Part 1*, 158–162. W. Szafer Institute of Botany, Polish Academy of Sciences, Kraków.

Lauterbach, S., Brauer, A., Andersen, N., Danielopol, D. L., Dulski, P., Hüls, M., Milecka, K., Namiotko, T., Obremska, M. & von Grafenstein, U. 2011: Environmental responses to Lateglacial climatic fluctuations recorded in the sediments of pre-Alpine Lake Mondsee (northeastern Alps). *Journal of Quaternary Science 26*, 253–267.

Leng, M. J. 2006: *Isotopes in Palaeoenvironmental Research*. 307 pp. Springer, Dordrecht.

Litt, T., Brauer, A., Goslar, T., Merkt, J., Bałaga, K., Müller, H., Ralska-Jasiewiczowa, M., Stebich, M. & Negendank, J. F. W. 2001: Correlation and synchronisation of Lateglacial continental sequences in northern central Europe based on annually laminated lacustrine sediments. *Quaternary Science Reviews 20*, 1233–1249.

Lotter, A. F. 1991: How long was the Younger Dryas? Preliminary evidence from annually laminated sediments of Soppensee (Switzerland). *Hydrobiologia 214*, 53–57.

Lücke, A. & Brauer, A. 2004: Biogeochemical and micro-facial fingerprints of ecosystem response to rapid Late Glacial climatic changes in varved sediments of Meerfelder Maar (Germany). *Palaeogeography, Palaeoclimatology, Palaeoecology 211*, 139–155.

Lücke, A., Schleser, G. H., Zolitschka, B. & Negendank, J. F. W. 2003: A Lateglacial and Holocene organic carbon isotope record of lacustrine palaeoproductivity and climatic change derived from varved lake sediments of Lake Holzmaar, Germany. *Quaternary Science Reviews 22*, 569–580.

Luoto, T. P., Kotrys, B. & Płóciennik, M. 2019: East European chironomid-based calibration model for past summer temperature reconstructions. *Climate Research 77*, 63–76.

Magny, M., Guiot, J. & Schoellammer, P. 2001: Quantitative reconstruction of Younger Dryas to Mid-Holocene paleoclimates at Le Locle, Swiss Jura, using pollen and lake-level data. *Quaternary Research 56*, 170–180.

Marciniak, B. & Szeroczyńska, K. 1998: Development of the Lake Gościąż biota during the Late-Glacial. *In* Ralska-Jasiewiczowa, M., Goslar, T., Madeyska, T. & Starkel, L. (eds.): *Lake Gościąż, Central Poland. A Monographic Study. Part 1*, 143–158. W. Szafer Institute of Botany, Polish Academy of Sciences, Kraków.

Marks, L., Gałązka, D. & Woronko, B. 2016: Climate, environment and stratigraphy of the last Pleistocene glacial stage in Poland. *Quaternary International 420*, 259–271.

Martin-Puertas, C., Brauer, A., Wulf, S., Ott, F., Lauterbach, S. & Dulski, P. 2014: Annual proxy data from Lago Grande di Monticchio (southern Italy) between 76 and 112 ka: new chronological constraints and insights on abrupt climatic oscillations. *Climate of the Past 10*, 2099–2114.

Neugebauer, I., Brauer, A., Dräger, N., Dulski, P., Wulf, S., Plessen, B., Mingram, J., Herzschuh, U. & Brande, A. 2012: A Younger Dryas varve chronology from the Rehwiese palaeolake record in NE-Germany. *Quaternary Science Reviews 36*, 91–102.

Pawłowski, D., Płóciennik, M., Brooks, S. J., Luoto, T. P., Milecka, K., Nevalainen, L., Peyron, O., Self, A. & Zieliński, T. 2015: A multiproxy study of Younger Dryas and Early Holocene climatic conditions from the Grabia River paleo-oxbow lake (central Poland). *Palaeogeography, Palaeoclimatology, Palaeoecology 438*, 34–50.

Peeters, F., Straile, D., Lorke, A. & Livingstone, D. M. 2007: Earlier onset of the spring phytoplankton bloom in lakes of the temperate zone in a warmer climate. *Global Change Biology 13*, 1898–1909.

Quinlan, R. & Smol, J. P. 2001: Setting minimum head capsule abundance and taxa deletion criteria in chironomid-based inference models. *Journal of Paleolimnology 26*, 327–342.

Rach, O., Brauer, A., Wilkes, H. & Sachse, D. 2014: Delayed hydrological response to Greenland cooling at the onset of the Younger Dryas in western Europe. *Nature Geoscience 7*, 109–112.

van Raden, U. J., Colombaroli, D., Gilli, A., Schwander, J., Bernasconi, S. M., van Leeuwen, J., Leuenberger, M. & Eicher, U. 2013: High-resolution late-glacial chronology for the Gerzensee lake record (Switzerland): δ¹⁸O correlation between a Gerzensee-stack and NGRIP. *Palaeogeography, Palaeoclimatology, Palaeoecology 391*, 13–24.

Ralska-Jasiewiczowa, M., Demske, D. & van Geel, B. 1998a: Late-Glacial vegetation history recorded in the Lake Gościąż sediments. *In* Ralska-Jasiewiczowa, M., Goslar, T., Madeyska, T. & Starkel, L. (eds.): *Lake Gościąż, Central Poland. A Monographic Study. Part 1*, 128–143. W. Szafer Institute of Botany, Polish Academy of Sciences, Kraków.

Ralska-Jasiewiczowa, M., van Geel, B. & Demske, D. 1998d: Holocene regional vegetation history recorded in the Lake Gościąż sediments. *In* Ralska-Jasiewiczowa, M., Goslar, T., Madeyska, T. & Starkel, L. (eds.): *Lake Gościąż, Central Poland. A Monographic Study. Part 1*, 202–219. W. Szafer Institute of Botany, Polish Academy of Sciences, Kraków.

Ralska-Jasiewiczowa, M., van Geel, B., Goslar, T. & Kuc, T. 1992: The record of the Late Glacial/Holocene transition in the varved sediments of lake Gosciaz, central Poland. *Sveriges Geologiska Undersökning, Ser. Ca 81*, 257–268.

Ralska-Jasiewiczowa, M., Goslar, T., Madeyska, T. & Starkel, L. 1998b: *Lake Gościąż, Central Poland. A Monographic Study. Part 1*. 340 pp. W. Szafer Institute of Botany, Polish Academy of Sciences, Kraków.

Ralska-Jasiewiczowa, M., Goslar, T., Madeyska, T. & Starkel, L. 1998c: Introduction. *In* Ralska-Jasiewiczowa, M., Goslar, T., Madeyska, T. & Starkel, L. (eds.): *Lake Gościąż, Central Poland. A Monographic Study. Part 1*, 10–16. W. Szafer Institute of Botany, Polish Academy of Sciences, Kraków.

Ralska-Jasiewiczowa, M., Goslar, T., Różański, K., Wacnik, A., Czernik, J. & Chróst, L. 2003: Very fast environmental changes at the Pleistocene/Holocene boundary, recorded in laminated sediments of Lake Gościąż, Poland. *Palaeogeography, Palaeoclimatology, Palaeoecology 193*, 225–247.

Ralska-Jasiewiczowa, M., Wicik, B. & Więckowski, K. 1987: Lake Gościąż - a site of annually laminated sediments covering 12000 years. *Bulletin of the Polish Academy of Sciences. Earth Sciences 35*, 127–137.

Ramisch, A., Brauser, A., Dorn, M., Blanchet, C., Brademann, B., Köppl, M., Mingram, J., Neugebauer, I., Nowaczyk, N., Ott, F., Pinkerneil, S., Plessen, B., Schwab, M.J., Tjallingii, R. & Brauer, A. 2020: VARDA (VArved sediments DAtabase) – providing and connecting proxy data from annually laminated lake sediments. *Earth System Science Data 12*, 2311–2332.

Ramisch, A., Tjallingii, R., Hartmann, K., Diekmann, B. & Brauer, A. 2018: Echo of the Younger Dryas in Holocene lake sediments on the Tibetan Plateau. *Geophysical Research Letters 45*, 11154–11163.

Rasmussen, S. O., Andersen, K. K., Svensson, A. M., Steffensen, J. P., Vinther, B. M., Clausen, H. B., Siggaard-Andersen, M.-L., Johnsen, S. J., Larsen, L. B., Dahl-Jensen, D., Bigler, M., Röthlisberger, R., Fischer, H., Goto-Azuma, K., Hansson, M. E. & Ruth, U. 2006: A new Greenland ice core chronology for the last glacial termination. *Journal of Geophysical Research: Atmospheres 111*, D06102, https://doi.org/10.1029/2005JD006079.

Rasmussen, S. O., Bigler, M., Blockley, S. P., Blunier, T., Buchardt, S. L., Clausen, H. B., Cvijanovic, I., Dahl-Jensen, D., Johnsen, S. J., Fischer, H., Gkinis, V., Guillevic, M., Hoek, W. Z., Lowe, J. J., Pedro, J. B., Popp, T., Seierstad, I. K., Steffensen, J. P., Svensson, A. M., Vallelonga, P., Vinther, B. M., Walker, M. J. C., Wheatley, J. J. & Winstrup, M. 2014: A stratigraphic framework for abrupt climatic changes during the Last Glacial period based on three synchronized Greenland ice-core records: refining and extending the INTIMATE event stratigraphy. *Quaternary Science Reviews 106*, 14–28.

Rasmussen, S. O., Vinther, B. M., Clausen, H. B. & Andersen, K. K. 2007: Early Holocene climate oscillations recorded in three Greenland ice cores. *Quaternary Science Reviews 26*, 1907–1914.

Rozanski, K., Klisch, M. A., Wachniew, P., Gorczyca, Z., Goslar, T., Edwards, T. W. D. & Shemesh, A. 2010: Oxygen-isotope geothermometers in lacustrine sediments: new insights through combined δ¹⁸O analyses of aquatic cellulose, authigenic calcite and biogenic silica in Lake Gościąż, central Poland. *Geochimica et Cosmochimica Acta 74*, 2957–2969.

Rychel, J., Woronko, B., Błaszkiewicz, M. & Karasiewicz, T. 2018: Aeolian processes records within last glacial limit areas based on the Płock Basin case (Central Poland). *Bulletin of the Geological Society of Finland 90*, 223–237.

Schenk, F., Bennike, O., Väliranta, M., Avery, R., Björck, S. & Wohlfarth, B. 2020: Floral evidence for high summer temperatures in southern Scandinavia during 15–11 cal ka BP. *Quaternary Science Reviews 233*, 106243, https://doi.org/10.1016/j.quascirev.2020.1.

Schenk, F., Väliranta, M., Muschitiello, F., Tarasov, L., Heikkilä, M., Björck, S., Brandefelt, J., Johansson, A. V., Näslund, J.-O. & Wohlfarth, B. 2018: Warm summers during the Younger Dryas cold reversal. *Nature Communications 9*, https://doi.org/10.1038/s41467-018-04071-5.

Schwander, J., Eicher, U. & Ammann, B. 2000: Oxygen isotopes of lake marl at Gerzensee and Leysin (Switzerland), covering the Younger Dryas and two minor oscillations, and their correlation to the GRIP ice core. *Palaeogeography, Palaeoclimatology, Palaeoecology 159*, 203–214.

Słowiński, M., Zawiska, I., Ott, F., Noryśkiewicz, A. M., Plessen, B., Apolinarska, K., Rzodkiewicz, M., Michczyńska, D. J., Wulf, S., Skubała, P., Kordowski, J., Błaszkiewicz, M. & Brauer, A. 2017: Differential proxy responses to late Allerød and early Younger Dryas climatic change recorded in varved sediments of the Trzechowskie palaeolake in Northern Poland. *Quaternary Science Reviews 158*, 94–106.

Starkel, L., Goslar, T., Ralska-Jasiewiczowa, M., Demske, D., Różański, K., Łącka, B., Pelisiak, A., Szeroczyńska, K., Wicik, B. & Więckowski, K. 1998: Discussion of the Holocene events recorded in the Lake Gościąż sediments. *In* Ralska-Jasiewiczowa, M., Goslar, T., Madeyska, T. & Starkel, L. (eds.): *Lake Gościąż, Central Poland. A Monographic Study. Part 1*, 239–246. W. Szafer Institute of Botany, Polish Academy of Sciences, Kraków.

Tjallingii, R., Röhl, U., Kölling, M. & Bickert, T. 2007: Influence of the water content on X-ray fluorescence core-scanning measurements in soft marine sediments. *Geochemistry, Geophysics, Geosystems 8*, Q02004, https://doi.org/10.1029/2006GC001393.

Weltje, G. J. & Tjallingii, R. 2008: Calibration of XRF core scanners for quantitative geochemical logging of sediment cores: theory and application. *Earth and Planetary Science Letters 274*, 423–438.

Weltje, G. J., Bloemsma, M. R., Tjallingii, R., Heslop, D., Röhl, U. & Croudace, I. W. 2015: Prediction of geochemical composition from XRF core scanner data: a new multivariate approach including automatic selection of calibration samples and quantification of uncertainties. *In* Croudace, I. & Rothwell, R. (eds.): *Micro-XRF Studies of Sediment Cores. Developments in Paleoenvironmental Research 17*, 507–534. Springer, Dordrecht.

Wójcik, G. & Przybylak, R. 1998: Present-day climatic conditions of the Lake Gościąż region. *In* Ralska-Jasiewiczowa, M., Goslar, T., Madeyska, T. & Starkel, L. (eds.): *Lake Gościąż, Central Poland. A Monographic Study. Part 1*, 22–26. W. Szafer Institute of Botany, Polish Academy of Sciences, Kraków.

Żarczyński, M., Wacnik, A. & Tylmann, W. 2019: Tracing lake mixing and oxygenation regime using the Fe/Mn ratio in varved sediments: 2000 year-long record of human-induced changes from Lake Żabińskie (NE Poland). *Science of the Total Environment 657*, 585–596.

Supporting Information

Additional Supporting Information may be found in the online version of this article at http://www.boreas.dk.

Fig. S1. Core correlation of the here observed interval of the composite profile GOS18 (Bonk *et al.* 2021).

Fig. S2. Lithology and microfacies data against composite depth.

Fig. S3. Selected microfacies data, XRF-data, $\delta^{13}C_{org}$, $\delta^{18}O_{carb}$ and chironomid-inferred mean July air temperature (MJAT) reconstruction using the East European Training Set (EE TS) against composite depth.

Fig. S4. $\delta^{13}C_{org}$, $\delta^{18}O_{carb}$, chironomid-inferred mean July air temperature (MJAT) reconstructions using the Swiss-Norwegian-Polish Training Set (SNP TS) (Kotrys *et al.* 2020) and the East European Training Set (EE TS) (Luoto *et al.* 2019) and detrended correspondence analysis (DCA) against composite depth.

Table S1. Marker layers (ML) of the here observed interval from the composite profile GOS18.

Table S2. Chironomid samples included in the mean July air temperature reconstruction with head capsule (hc) counts below 50.